Spin dynamics in a finite cyclic XY model

Evgeniy Safonov[1] and Oleg Lychkovskiy[1,2]
[1]*Institute for Theoretical and Experimental Physics B. Cheremushkinskaya 25, 117218 Moscow, Russia*
[2]*Physics Department, Lancaster University, Lancaster LA1 4YB, United Kingdom*
(Received 19 June 2012; published 9 April 2013)

Evolution of the z component of a single spin in a finite cyclic XY spin-1/2 chain is studied. Initially one selected spin is polarized while other spins are completely unpolarized and uncorrelated. Polarization of the selected spin as a function of time is proportional to the autocorrelation function $g_0^{zz}(t)$ at infinite temperature. Initialization of the selected spin gives rise to two wave packets moving in opposite directions and winding over the circle. We express $g_0^{zz}(t)$ as a series in winding number and derive tractable approximations for each term. This allows us to give qualitative explanations and quantitative descriptions of various finite-size effects such as partial revivals and transition from regular to erratic behavior.

DOI: 10.1103/PhysRevA.87.042105 PACS number(s): 03.65.Yz, 02.30.Ik

I. INTRODUCTION

Exactly solvable spin chains are widely used as toy models for exploring various aspects of quantum dynamics. Recent progress in experimental techniques allows the construction of quantum systems with effective spin chain Hamiltonians (see, e.g., [1]), which opens new prospects for exploration of fundamental concepts such as decoherence and thermalization, as well as for applications such as quantum state transfer through quantum wires [2]. This motivates further efforts to understand dynamics of spin chains in detail.

We consider the reduced dynamics of a single spin in a cyclic spin 1/2 XY chain with a finite number of spins, N. Initially one selected spin has a given polarization while other $(N-1)$ spins are completely uncorrelated and unpolarized. We study the z component of polarization of the selected spin as a function of time. It can be expressed through the time-dependent autocorrelation functions $g_0^{zz}(t)$. Although many papers, starting from the pioneering paper on the XY chain [3], have been devoted to calculation of various correlation functions, most of the studies have concentrated on the thermodynamic limit $N \to \infty$. An exact expression for $g_0^{zz}(t)$ in the XY model with finite N was derived in [4] and [5]. It involves sums of $\sim N$ oscillating terms and thus is hardly tractable. However, these sums can be calculated numerically for various values of model parameters. Resulting plots for $g_0^{zz}(t)$ readily reveal a rich variety of spin evolution patterns which call for explanation (see the figures in the present paper, especially Fig. 1). One striking feature of the evolution is the regular-to-erratic transition: $g_0^{zz}(t)$ is described fairly well by $N \to \infty$ approximation (which is given by a rather regular function of time for a wide range of model parameters) up to some threshold time t_{th}, but at t_{th} this concordance is abruptly destroyed by a sharp revival; at later times the evolution becomes less and less regular and ends up with apparently chaotic fluctuations near the long-time average. This feature is apparently common for all finite spin chains; in particular, it was observed in numerical simulations done for the XX (isotropic XY) model [6,7], for the XXZ model with long-range [8] and nearest-neighbor [9] couplings, and for the XY model [10].

Results of the numerical studies and general considerations suggest that it is the winding of two oppositely directed wave packets created by the spin initialization which underlies the long-time dynamics in the cyclic chain [7] (in the case of an open-ended chain the same role is played by the reflection of the packets from the ends of the chain [6]). The threshold time corresponds to the time necessary for the forefront of a wave packet to make one round-trip over the circle.[1] The interference between the forefronts of the wave packets and their own tails produces partial revivals at $t = t_{\text{th}}, 2t_{\text{th}}, \ldots$ and leads to the regular-to-erratic transition.

In order to study spin dynamics in finite spin chains at times greater than t_{th} it is desirable to have tractable analytical approximations for $g_0^{zz}(t)$ valid for $t > t_{\text{th}}$. The main goal of the present paper is to obtain such approximations for the cyclic XY model. The mathematical method which we use and develop is closely related to the physical picture of wave-packet winding over the circle and in fact allows us to quantitatively describe such winding. Namely, we are able to represent the correlation function as a series in winding number s. This series has the appealing property that $(s+1)$ first terms are enough to describe the correlation function for $t < (s+1)t_{\text{th}}$. Such a truncated series fully takes into account interference between the components of the wave packets which have completed $0, 1, 2, \ldots, s$ round-trips over the circle. These approximations are fairly accurate even when the evolution is already completely irregular. Related results in this direction were previously obtained in Refs. [12,13]. In Ref. [12] a quasiparticle Green's function was represented as a sum over winding numbers. Recently the method was applied to the inhomogeneous open-ended XX chain [13,14]. Similar mathematical structures and physical patterns emerge in systems of coupled oscillators (see, e.g., Ref. [15] and references therein).

The approximation accounting for s windings involves $\sim s$ oscillating terms and therefore is much more tractable than the exact formula as long as $s \ll N$. This allows us to look at the regular-to-erratic transition (as well as some other peculiar features of spin evolution in finite chains) from a different perspective and obtain quantitative results hardly accessible in

[1]See also a recent paper [11] for the same physical reasoning applied to dynamics after a quench in the XY model.

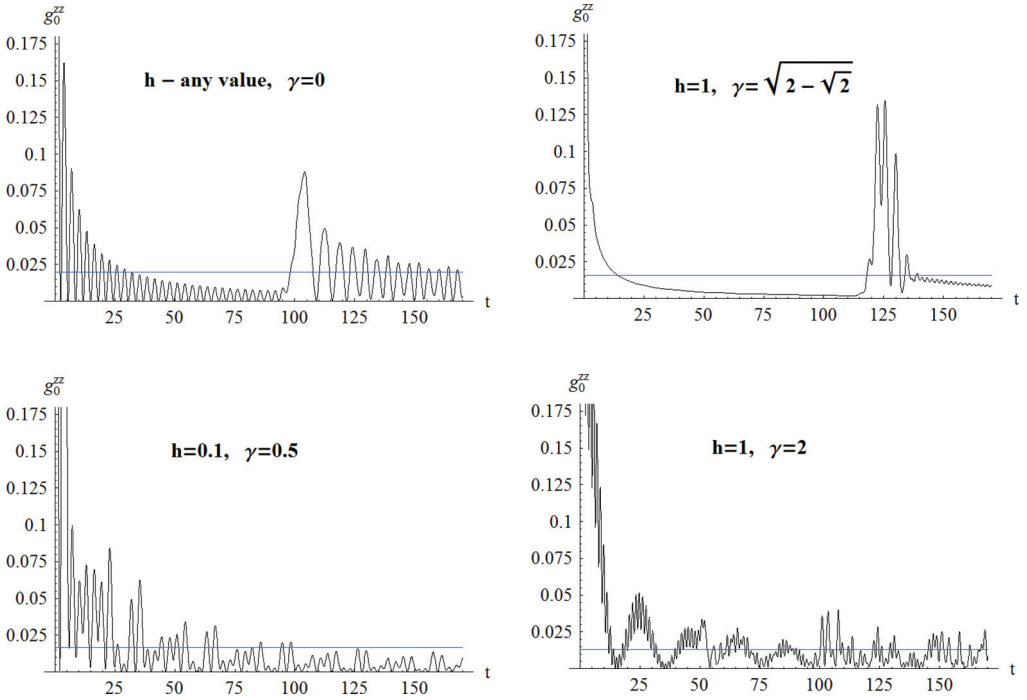

FIG. 1. (Color online) Patterns of spin dynamics for various values of model parameters. The exact autocorrelation function $g_0^{zz}(t)$ is plotted. According to Eq. (9) it is equal to the polarization of the first spin $p_1^z(t)$ provided $p_1^z(0) = 1$. The horizontal (blue) line marks the long-time average of the autocorrelation function given by Eq. (B10). The number of spins here and in all other figures is $N = 100$.

numerical simulations. For example, we are able to derive an asymptotic formula for the amplitude of the sth revival.

We also touch on the issue of incomplete thermalization of spins in the XY spin chain. In particular, we show that the autocorrelation function $g_0^{zz}(t)$ at infinite temperature never changes its sign, in contrast to what would be expected in the case of complete thermalization. This intriguing property was previously proven in the special case of the XX chain [6,7] and observed in numerical calculations of spin evolution in the XXZ model with long-range interactions [8].

The rest of the paper is organized as follows. In Sec. II we briefly describe the XY model on a circle. In Sec. III we discuss the exact formula for $g_0^{zz}(t)$ and rewrite it through sums over winding numbers. In two special cases (the Ising model with a critical magnetic field and the XX model) this directly leads to the desired result: $g_0^{zz}(t)$ is represented in a transparent and convenient way through the infinite sum of Bessel functions. This representation allows us to obtain simple successive approximations valid up to times $t_{\rm th}, 2t_{\rm th}, \ldots$. However, in the general case each term of the sum is represented as an integral which should be worked out. In Sec. IV we handle these integrals approximately. Thus we obtain our main result: the successive asymptotic approximations in a general case. In Sec. V we discuss the transition from regular to erratic behavior. The results are summarized in Sec. VI. The bulk of the technical details is presented in the Appendixes. In Appendix A we describe the diagonalization of the XY model. In Appendix B we rederive the exact formula for the correlation function $g_n^{zz}(t)$ at infinite temperature using a method which is somewhat more direct than the one implemented in the original work [4,5]. These two appendixes mostly contain widely known calculations and results; however, we include them in order to introduce our notations, to emphasize some salient features usually omitted in the literature and for the sake of completeness. In Appendix C the dependence of the wave-packet forefront velocity on the model parameters is investigated. Appendix D contains the technical details of calculating asymptotic expressions presented in Sec. IV.

II. THE XY MODEL ON A CIRCLE

We consider a chain of N coupled spin-1/2's with the following Hamiltonian [3,16]:

$$H = \frac{1}{4}\sum_{n=1}^{N}\left[(1+\gamma)\sigma_n^x\sigma_{n+1}^x + (1-\gamma)\sigma_n^y\sigma_{n+1}^y\right] + \frac{h}{2}\sum_{n=1}^{N}\sigma_n^z. \tag{1}$$

Here the index $N+1$ is identified with 1, and N is supposed to be even. Two parameters enter the Hamiltonian, the anisotropy parameter γ and the magnetic field h. Without loss of generality one may assume $\gamma \geqslant 0$, $h \geqslant 0$ (see Appendix A). In Sec. IV we concentrate on the case $h \geqslant 1$, $\gamma \in [0,1]$.

An important property of the XY Hamiltonian is that it commutes with the parity operator $\Pi \equiv \prod_{n=1}^{N}\sigma^z$. It can be represented in an "almost-free-fermion form" through the sequential Jordan-Wigner, Fourier, and Bogolyubov transformations [3–5] (see Appendix A for details):

$$H = P^{\rm odd}\sum_{q\in X_{\rm odd}} E_q\left(c_q^+c_q - \frac{1}{2}\right) + P^{\rm ev}\sum_{q\in X_{\rm ev}} E_q\left(c_q^+c_q - \frac{1}{2}\right), \tag{2}$$

where

$$X_{\rm odd} = \left\{-\frac{N}{2}+1,-\frac{N}{2}+2,\ldots,\frac{N}{2}\right\},$$
$$X_{\rm ev} = \left\{-\frac{N}{2}+\frac{1}{2},-\frac{N}{2}+\frac{3}{2},\ldots,\frac{N}{2}-\frac{1}{2}\right\}, \tag{3}$$

$\{c_q, q \in X_{\rm odd}\}$ and $\{c_q, q \in X_{\rm ev}\}$ are two sets of fermion operators [note, however, that two operators from different sets do not satisfy fermion anticommutation relations; see Eq. (A21)], $P^{\rm odd}$ and $P^{\rm ev}$ are parity projectors,

$$P^{\rm ev} \equiv (1+\Pi)/2, \quad P^{\rm odd} \equiv (1-\Pi)/2, \tag{4}$$

and the fermion energy is defined as $E_q \equiv E(\varphi(q))$, $\varphi(q) \equiv \frac{2\pi q}{N}$,

$$E(\varphi) = \sqrt{\varepsilon(\varphi)^2+\Gamma(\varphi)^2}, \quad \varepsilon(\varphi) \equiv h - \cos\varphi,$$
$$\Gamma(\varphi) \equiv \gamma \sin\varphi. \tag{5}$$

One can see that the Hilbert space is divided into two subspaces, with odd and even numbers of fermions, respectively. The number of fermions is an integral of motion, and when it is fixed, the model looks like a free-fermion model.

III. REDUCED DYNAMICS OF A SPIN AT $T = \infty$

A. Correlation function: Sum over modes

We focus our study on the z component of the nth spin polarization vector as a function of time:

$$p_n^z(t) \equiv {\rm tr}\left[\rho(t)\sigma_n^z\right], \tag{6}$$

where $\rho(t) = e^{-iHt}\rho(0)e^{iHt}$ is the density matrix of the whole chain.

We choose the following initial condition:

$$\rho(0) = 2^{-N}[\mathbb{1}_1 + \mathbf{p}_1(0)\boldsymbol{\sigma}_1] \otimes \mathbb{1}_{23\ldots N}. \tag{7}$$

It describes a situation where at $t = 0$ the first spin has an arbitrary polarization, $\mathbf{p}_1(0)$, while other $(N-1)$ spins are completely unpolarized and uncorrelated. If the first spin is regarded as an open system, and other $(N-1)$ spins as an environment, then this initial condition corresponds to an infinite temperature of the environment. Given the above initial condition, the polarization $p_n^z(t)$ can be expressed through the two-spin correlation functions at infinite temperature, $p_n^z(t) = p_1^\alpha(0) g_{n-1}^{z\alpha}(t)$, where

$$g_n^{z\alpha}(t) \equiv 2^{-N}{\rm tr}\left[\sigma_{n+1}^\alpha(t)\sigma_1^z\right]. \tag{8}$$

Due to conservation of parity $g_n^{zx}(t) = g_n^{zy}(t) = 0$ and we are left with

$$p_n^z(t) = p_1^z(0) g_{n-1}^{zz}(t). \tag{9}$$

Note that this relation between the polarization of a single spin and the correlation function holds only in the case of infinite temperature.

Thus our problem reduces to investigation of the zz correlation function g_n^{zz}. Due to integrability of the model it can be calculated exactly [4,5]. For completeness of the presentation we provide the details of the calculation in Appendix B. The result reads

$$g_n^{zz}(t) = \tfrac{1}{2}\left(A_{\rm odd}^{n\ 2} + A_{\rm ev}^{n\ 2} + B_{\rm odd}^{n\ 2} + B_{\rm ev}^{n\ 2} - C_{\rm odd}^{n\ 2} - C_{\rm ev}^{n\ 2}\right), \tag{10}$$

where

$$A^n_{\rm ev(odd)}(t) = N^{-1}\sum_{q\in X_{\rm ev(odd)}} \cos n\varphi(q)\cos E_q t,$$
$$B^n_{\rm ev(odd)}(t) = N^{-1}\sum_{q\in X_{\rm ev(odd)}} \frac{\varepsilon_q}{E_q}\cos n\varphi(q)\sin E_q t, \tag{11}$$
$$C^n_{\rm ev(odd)}(t) = N^{-1}\sum_{q\in X_{\rm ev(odd)}} \frac{\Gamma_q}{E_q}\sin n\varphi(q)\sin E_q t.$$

In what follows we mainly concentrate on the evolution of the first spin, which is distinguished by the initial condition. It is described by the autocorrelation function $g_0^{zz}(t)$.

As noted in [7], in the case of the XX model ($\gamma = 0$), $g_n^{zz}(t)$ is always non-negative [because $C^n_{\rm ev(odd)}(t) = 0$] or, in other words, spin polarization never changes its sign. We see that this is not the case for an arbitrary site n in a general XY chain. However, the polarization of the first spin still never changes its sign since $C^0_{\rm ev(odd)}(t) = 0$ for any γ. Intriguingly, the same property [non-negativity of $g_0^{zz}(t)$ at infinite temperature] was observed in numerical simulations for the XXZ model with long-range interactions [8]. This suggests that this effect could be generic for a large class of spin systems.

Surprisingly enough, the evolution of spin polarization described by the exact formula, (10), exhibits a rich variety of patterns depending on h and γ. Examples are given in Fig. 1. We aim at explaining the major features of evolution and at providing a tractable approximation to Eq. (10).

B. Correlation function: Sum over winding numbers

Let us rewrite formulas (11) for $n = 0$ in a different form:

$$A^0_{\rm odd}(t) = A_0(t) + 2\sum_{j=1}^{\infty} A_j(t),$$
$$A^0_{\rm ev}(t) = A_0(t) + 2\sum_{j=1}^{\infty}(-1)^j A_j(t),$$
$$B^0_{\rm odd}(t) = B_0(t) + 2\sum_{j=1}^{\infty} B_j(t), \tag{12}$$
$$B^0_{\rm ev}(t) = B_0(t) + 2\sum_{j=1}^{\infty}(-1)^j B_j(t),$$

where

$$A_j(t) \equiv (2\pi)^{-1}{\rm Re}\int_{-\pi}^{\pi} e^{{\rm i}(E(\varphi)t - jN\varphi)}d\varphi,$$
$$B_j(t) \equiv (2\pi)^{-1}{\rm Im}\int_{-\pi}^{\pi} \frac{\varepsilon(\varphi)}{E(\varphi)} e^{{\rm i}(E(\varphi)t - jN\varphi)}d\varphi. \tag{13}$$

As shown below, j corresponds to a number of windings of the forefront of a wave packet produced by the initialization of the first spin. To obtain the above expressions one should take a discrete Fourier transform of the right-hand side (r.h.s.)

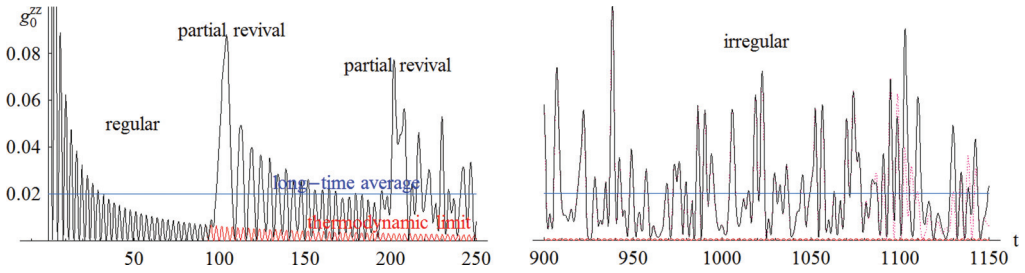

FIG. 2. (Color online) $g_0^{zz}(t)$ for the XX model. The threshold time is $t_{\rm th} = N = 100$. The solid line corresponds to the exact expression. The dotted (magenta) line corresponds to approximation (17) with $j = 0,1,\ldots,10$. One can see that the approximation starts to deviate from the exact expression only at $t \simeq 11t_{\rm th}$. The approximation obtained in the thermodynamic limit ($j = 0$) is also shown (in red). It accurately describes $g_0^{zz}(t)$ up to the threshold time. The horizontal (blue) line marks the long-time average of the autocorrelation function.

of Eq. (11) and use

$$\sum_{q\in X_{\rm odd}} e^{il\varphi(q)} = \begin{cases} 1 & \text{if} \quad l = jN, \quad j \in Z, \\ 0 & \text{otherwise;} \end{cases}$$
$$\sum_{q\in X_{\rm ev}} e^{il\varphi(q)} = \begin{cases} (-1)^j & \text{if} \quad l = jN, \quad j \in Z, \\ 0 & \text{otherwise.} \end{cases} \tag{14}$$

Formulas (12) have an important advantage compared to formulas (11): infinite sums in (12) can be truncated at some small j to obtain excellent approximations for times $t < (j+1)t_{\rm th}$ with threshold time $t_{\rm th} \sim N$. Thus one may deal with only a few terms in Eq. (12), in contrast to N terms in (11). This statement is proved in full generality in the following (see Sec. IV and, especially, Appendix D 2b). In two special cases described below one can check it immediately.

C. Special case: The XX chain

When $\gamma = 0$ functions A_j and B_j can be expressed through Bessel functions of the first kind,

$$A_j(t) = (-1)^{Nj/2}\cos(ht)J_{jN}(t),$$
$$B_j(t) = (-1)^{Nj/2}\sin(ht)J_{jN}(t). \tag{15}$$

$J_{jN}(t)$ is negligible for $t < jN$, which justifies the truncation of the sums in (12). The threshold time in this case equals N.

In fact in the case of the XX chain Eq. (10) may be further simplified to obtain

$$g_0^{zz}(t) = \frac{1}{2}\left[\left(J_0(t) + 2\sum_{j=1}^{\infty} J_{jN}(t)\right)^2 + \left(J_0(t) + 2\sum_{j=1}^{\infty}(-1)^j J_{jN}(t)\right)^2\right] = \sum_{j+j'=0(\mathrm{mod}\,2)} J_{jN}(t)J_{j'N}(t). \tag{16}$$

Note that h drops out of the final expression. This can be easily seen from the definition, (8), of $g_n^{zz}(t)$ if one recalls that $\frac{h}{2}\sum_n \sigma_n^z$ commutes with the total Hamiltonian.[2]

Equation (16) may be used to obtain successive approximations:

$g_0^{zz}(t) \simeq$	For $t \in$
$J_0^2(t)$	$[0,N)$
$J_0^2(t) + 4J_N^2(t)$	$[N,2N)$
$J_0^2(t) + 4J_N^2(t) + 4J_{2N}^2(t) + 4J_0(t)J_{2N}(t)$	$[2N,3N)$
$\ldots$	

(17)

The first line ($j = 0$) represents a well-known result obtained in the thermodynamic ($N \to \infty$) limit [16]. Approximations in which $(s+1)$ Bessel functions are kept correspond to s round-trips of a spin wave over the circle. We postpone further discussion of the physical sense of the obtained results until the next section. Exact and approximate expressions for $g_0^{zz}(t)$ in the XX chain are plotted in Fig. 2.

Closely related results for the XX model were obtained in Ref. [12] and in Refs. [13,14]. In Ref. [12] the one-particle Green function [which is in fact equal to the *zero-temperature* correlation function $g_n^{-+}(t)|_{T=0} \equiv \langle\downarrow\downarrow\ldots\downarrow|\sigma_{n+1}^-(t)\sigma_1^+|\downarrow\downarrow\ldots\downarrow\rangle$] was represented as an infinite sum of Bessel functions. In Refs. [13,14] an open-ended XX chain with an impurity in the center was considered, the impurity coupling being, in general, different from the bulk coupling; again, the zero-temperature autocorrelation function was represented as a sum over cycle number.

D. Special case: The Ising chain with $h = 1$

In the case $h = 1$, $\gamma = 1$, one obtains

$$A_j(t) = J_{2jN}(2t),$$
$$B_j(t) = \tfrac{1}{2}(J_{2jN+1}(2t) - J_{2jN-1}(2t)) = -J'_{2jN}(2t), \tag{18}$$

where the prime stands for the derivative. Again, $A_j(t)$ and $B_j(t)$ are negligible for $t < jt_{\rm th}$ with $t_{\rm th} = N$. Successive

[2] As Professor Perk noted in a private communication, another way to explain this fact is to use the transformation into the rotating frame, a procedure familiar from the theory of magnetic resonance.

TABLE I. Value of the maximal group velocity V in some special cases.

		$\gamma = 1$			$h = 1$		$h = 1$,
	$\gamma = 0$	$h < 1$	$h \geqslant 1$	$h = 0$	$\gamma^2 \in [0,3/4)$	$\gamma^2 \in [3/4,1]$	$\gamma = \sqrt{2-\sqrt{2}}$
$\cos\varphi_0$	0	h	$1/h$	$-\sqrt{\frac{\gamma}{1+\gamma}}$	$\frac{2\gamma^2+1-\sqrt{4\gamma^2+1}}{2(1-\gamma^2)}$	1	~ 0.414
V	1	h	1	$1-\gamma$	—[a]	γ	$2(\sqrt{2}-1)$

[a]A bulky (although explicit) expression, see Appendix C for details.

approximations can be written analogously to the XX case discussed above.

IV. ASYMPTOTIC APPROXIMATIONS

In the present section we derive asymptotic approximations for functions A_j and B_j which enter Eq. (12). As we will see, these approximations physically correspond to taking into account spin waves which wind over a circle j times. The details of the calculations are presented in Appendix D. Here we outline only major results, emphasizing their physical meaning. In the present section we restrict our study to the case $h \geqslant 1$, $\gamma \in [0,1]$.

A. Winding of a wave packet over a circle

We approximately calculate $A_j(t)$ and $B_j(t)$ using the method of the steepest descent in the plane of a complex variable φ. The saddle points for A_j are obtained from the equation

$$v(\varphi)t - jN = 0, \tag{19}$$

where $v(\varphi) \equiv \partial_\varphi E$ is the group velocity corresponding to momentum φ [the equation corresponding to B_j is slightly different; see Eq. (D3) in Appendix D]. Note that, in general, the positions of saddle points depend on time (to be more exact, on the ratio t/jN). Two important cases should be distinguished, $t < jt_{\rm th}$ and $t > jt_{\rm th}$, where $t_{\rm th} \equiv N/V$ and $V \equiv \sup_\varphi v(\varphi) = v(\varphi_0)$. In the former case Eq. (19) has no real roots, and as a consequence, $A_j(t)$ and $B_j(t)$ are severely suppressed (in accordance with a general result [17]). This explains why one can keep only j terms in Eq. (12) whenever $t < jt_{\rm th}$. If h is not too close to 1, the suppression law reads

$$A_j(t), B_j(t) \sim \exp\left[-\text{const} \times jN\left(\frac{jt_{\rm th}-t}{jt_{\rm th}}\right)^{\frac{3}{2}}\right], \quad t < jt_{\rm th}, \tag{20}$$

where the constant is of the order of 1 and depends on h and γ (see Appendix D 2b).

In the opposite case, $t > jt_{\rm th}$, Eq. (19) has two real roots and $A_j(t)$ and $B_j(t)$ are not suppressed.

The threshold time $t_{\rm th}$ is the time which is necessary for the fastest spin wave to make one round-trip over the circle [7]. Thus $A_j(t)$ and $B_j(t)$ describe the contributions of those parts of the wave packet which have completed exactly j round-trips over the circle. The propagation of the wave packet is visualized in Fig. 3 (see also an analogous figure for the XX model in [7]). As shown in [7], the initial excitation of the first spin gives rise to two wave packets which travel in opposite directions. Each wave packet is a superposition of all spin waves of corresponding direction. The velocity of the forefronts of these wave packets coincides with the maximal group velocity of the spin waves V. Therefore as long as $t < t_{\rm th} \equiv N/V$, the wave packets propagate as if the chain were infinite, and the evolution of the first spin is described merely by oscillations in the common tail of the wave packets. This stage of evolution is the only one which may be catched by the $N \to \infty$ approximation. Mathematically it is described by keeping only $j = 0$ terms in Eq. (12).

At $t = t_{\rm th}$ the forefronts of two wave packets complete the round-trip over the circle and meet at the first site. At this moment the regular evolution of the polarization of the first spin is abruptly interrupted by a partial revival. The succeeding evolution between $t_{\rm th}$ and $2t_{\rm th}$ is determined by the interference between the fastest parts of wave packets which have already made one round-trip and the common tail of the wave packets with zero velocity, which still stays at the first site. Mathematically this stage is described by keeping $j = 0,1$ terms in Eq. (12).

Subsequent stages are described in a similar fashion. The wave packets continue to wind over the circle. At $st_{\rm th} < t < (s+1)t_{\rm th}$, polarization at the first site is the result of interference of waves which have completed $0,1,\ldots,s$ round-trips over the circle. This corresponds to keeping $j = 0,1,\ldots,s$ terms in Eq. (12). The revivals at $t = st_{\rm th}$ become less pronounced with increasing s due to the decrease in the maximal amplitude and the smearing of the forefront of the wave packet (see Fig. 3).

Clearly the maximal group velocity V is an important quantity in the above picture, as it determines the threshold time. We show in Appendix C that $V \in [2(\sqrt{2}-1),1]$ as long as we restrict ourselves to the case $h \geqslant 1$. Without this restriction, V is confined to the interval $[0,1]$. $V = 2(\sqrt{2}-1)$ is achieved at $h = 1$, $\gamma = \sqrt{\sqrt{2}-1}$ (this case is presented in the upper right plot in Fig. 1 and on Fig. 3). More detailed considerations can be found in Appendix C. Values of V in some important specific cases are listed in Table I.

The above-described physical picture of propagation of wave packets and emergence of revivals implies that the forefront of the wave packet is rather sharp. This is indeed true, for the following simple reason. As long as φ_0 is a point of maximum, a bunch of fermions exists, with $\varphi(q)$ lying in the vicinity of φ_0. The group velocities of these modes are equal to each other and to the maximal velocity V up to quadratic terms. It it is exactly these modes which form the sharp forefront of the wave packet, which smears very slowly compared to the rest of the wave packet. Some proposals for

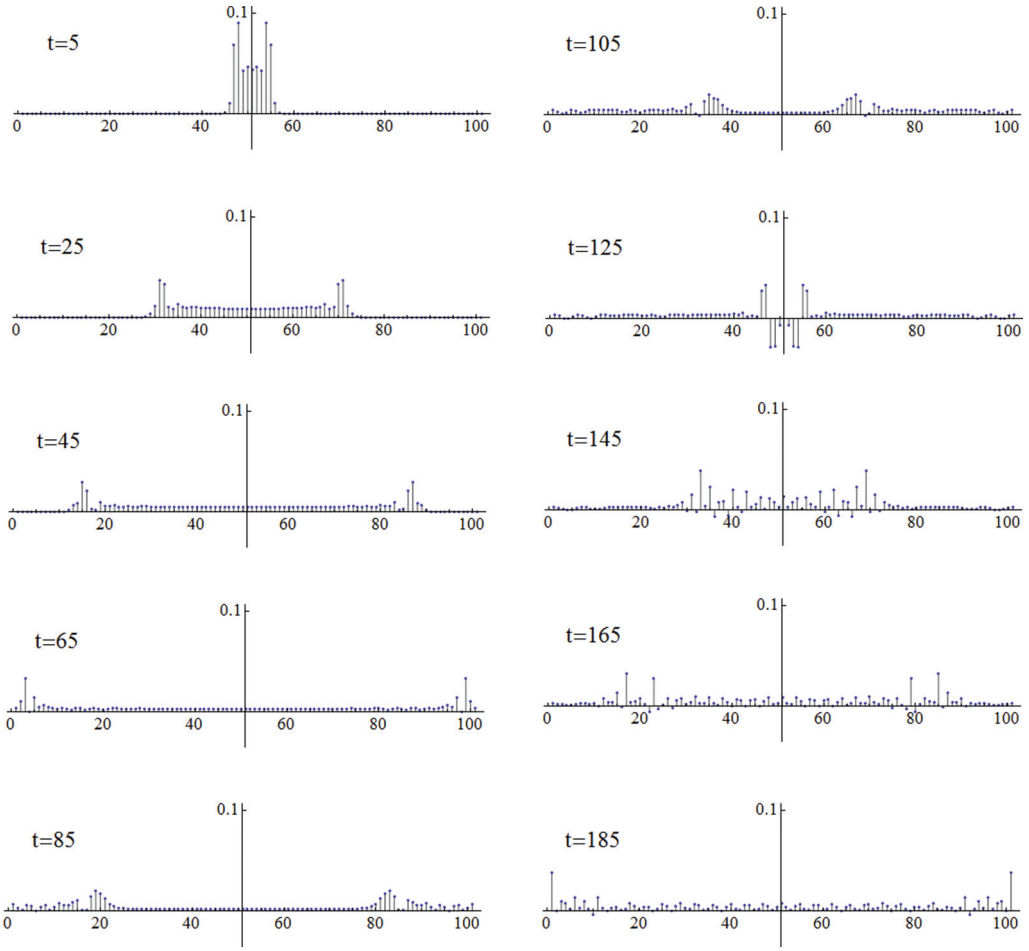

FIG. 3. (Color online) Propagation of two oppositely directed wave packets along a spin chain. Snapshots of polarizations of all spins at times $t = 5,25,\ldots,185$ are presented. The initial spin excitation is localized at the 51st site here (in contrast to the rest of the paper); the 0th site is identified with the 100th one. The model parameters are $h = 1$ and $\gamma = \sqrt{\sqrt{2}-1}$, and the threshold time is $t_{\rm th} \simeq 117.7$. Note the emergence of a polarization plateau, which increases up to $t_{\rm th}/2$, then shrinks and completely disappears at the threshold time. This feature is specific for the case $h = 1$. A three-dimensional plot representing a more generic case (without a plateau) of propagation of wave packets along the cyclic XX chain can be found in [7].

high-quality quantum state transfer along spin chains exploit this feature (see, e.g., [18]).

B. Asymptotic approximations for $t < t_{\rm th}$

First, we separately consider the case $t < t_{\rm th}$ (see Appendix D 1). This case is special because the positions of saddle points do not depend on time. Approximations in this time interval coincide with formulas obtained in the thermodynamic limit.

Let us introduce a dimensionless parameter $\epsilon \equiv h - 1$. Here and in what follows we mainly concentrate on the case where h is not too close to 1. In this case the method of the steepest descent can be applied straightforwardly, and we obtain an asymptotic approximation for times $\max\{1,\epsilon^{-1}\} < t < t_{\rm th}$:

$$g_0^{zz}(t) \simeq \frac{1}{2\pi t}\left[(a_{0+}-a_{0-})^2 + 4a_{0+}a_{0-}\cos^2\left(t-\frac{\pi}{4}\right)\right], \tag{21}$$

where

$$a_{0\pm} \equiv \sqrt{\frac{h\pm 1}{h\pm(1-\gamma^2)}}.$$

Note that ϵ should be greater than N^{-1}; otherwise the time interval at which the approximation is valid vanishes. This restriction is relaxed if $\gamma \ll \epsilon$. In the latter case even for $\epsilon \ll 1$ formula (21) is valid for $1 \ll t < t_{\rm th}$. In fact in this case one can approximate $g_0^{zz}(t)$ simply by the autocorrelation function for $\gamma = 0$, which is given by $J_0^2(t)$ for $t < t_{\rm th}$ according to (17).

In the case of small ϵ the application of the method of the steepest descent is more sophisticated. The complications are not unexpected because $h = 1$ is the point of quantum phase transition (QPT) for the XY model. However, given certain relations among ϵ, γ, and N^{-1}, one may still obtain accurate approximations (see Appendix D 1). For example, in the case $\epsilon^2 \lesssim \gamma^2 \ll 1$ we are able to obtain an asymptotic expression

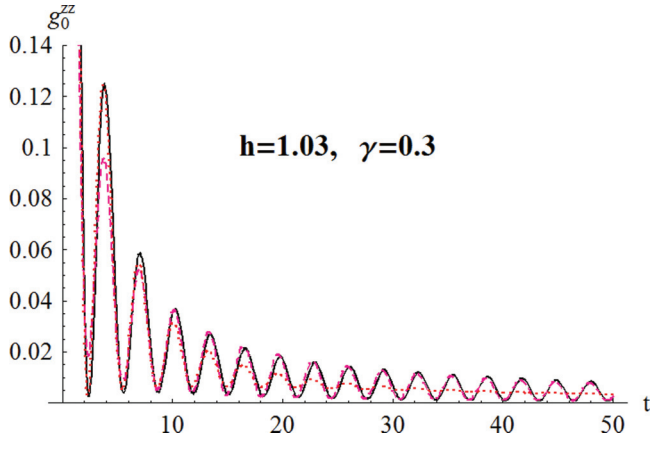

FIG. 4. (Color online) Autocorrelation function $g_0^{zz}(t)$ at $t < t_{\rm th}$ or, equivalently, in the thermodynamic limit. Solid line, exact expression; dashed (magenta) line, asymptotic approximation (21) valid for lager times, $\epsilon^{-1} < t < t_{\rm th}$; dotted (red) line, asymptotic approximation (22) valid for smaller times, $1 < t \ll \gamma^2\epsilon^{-2}$.

valid for $1 < t \ll \gamma^2\epsilon^{-2}$:

$$g_0^{zz}(t) \simeq \frac{1}{\pi(2-\gamma^2)t}\left(1+\frac{2-\gamma^2}{2\sqrt{1-\gamma^2}}\exp\left[-\frac{2\gamma^2}{\sqrt{1-\gamma^2}}t\right]+2\sqrt{\frac{2-\gamma^2}{2\sqrt{(1-\gamma^2)}}}\exp\left[-\frac{\gamma^2}{\sqrt{1-\gamma^2}}t\right]\times\cos\left(2t-\frac{\pi}{4}-\arctan\frac{1}{\sqrt{1-\gamma^2}}\right)\right). \quad (22)$$

If γ is not too small, the exponents rapidly decrease with time and one is left with nonoscillating decay:

$$g_0^{zz}(t) = \frac{1}{\pi(2-\gamma^2)t}. \quad (23)$$

For certain values of parameters both asymptotic approximations, (21) and (22), may be applicable, but at different time intervals. An example is given in Fig. 4.

C. Asymptotic approximations for $t > jt_{\rm th}$

Now let us turn to asymptotics for functions $A_j(t)$ and $B_j(t)$ and corresponding approximations for $g_0^{zz}(t)$ in the case of $j \geqslant 1$. It has been already noted that $A_j(t)$ and $B_j(t)$ are suppressed for $t < jt_{\rm th}$.

For sufficiently long times and h not too close to 1 [more explicitly, for $(t - jt_{\rm th}) \gg 1$ and $\epsilon^{-1} \ll jt_{\rm th}$], we obtain (see Appendix D 2a)

$$A_j(t) \simeq \frac{1}{\sqrt{2\pi t}}\left(\sqrt{\frac{1}{|E''(\varphi_1)|}}\cos\left(tE(\varphi_1)-jN\varphi_1+\frac{\pi}{4}\right)+\sqrt{\frac{1}{|E''(\varphi_2)|}}\cos\left(tE(\varphi_2)-jN\varphi_2-\frac{\pi}{4}\right)+O\left(\frac{1}{t}\right)\right), \quad (24)$$

$$B_j(t) \simeq \frac{1}{\sqrt{2\pi t}}\left(\sqrt{\frac{1}{|E''(\varphi_1)|}}\frac{\varepsilon(\varphi_1)}{E(\varphi_1)}\sin\left(tE(\varphi_1)-jN\varphi_1+\frac{\pi}{4}\right)+\sqrt{\frac{1}{|E''(\varphi_2)|}}\frac{\varepsilon(\varphi_2)}{E(\varphi_2)}\sin\left(tE(\varphi_2)-jN\varphi_2-\frac{\pi}{4}\right)+O\left(\frac{1}{t}\right)\right). \quad (25)$$

Saddle points $\varphi_{1,2}(t)$ are obtained from Eq. (19). The latter may be reduced to a polynomial equation, (D16), of fourth degree with regard to $\cos\varphi$.

These asymptotics, plugged into Eq. (12), excellently approximate $g_0^{zz}(t)$ everywhere but in the vicinity of points $jt_{\rm th}$, where revivals occur. In order to describe revivals one should use different approximate expressions presented in the next subsection.

The case of small ϵ is, again, more cumbersome. However, it can also be treated as demonstrated in Appendix D 2a.

D. Partial revivals

The above-derived approximations based on the method of the steepest descent are not applicable in the vicinity of multiples of $t_{\rm th}$ when two saddle points are close to each other and to the point φ_0. However, as long as at $t = jt_{\rm th}$ is exactly the time at which a partial revival occurs, it is highly desirable to have an approximation which works well for $t \simeq jt_{\rm th}$. We derive such an approximation in Appendix D 2c. The derivation is based on the fact that in the case under consideration the integrals in the definitions (13) of A_j and B_j pick up the major contribution in the vicinity of φ_0. This justifies the expansion of $E(\varphi)$ in the vicinity of φ_0, which leads to the desired approximate expressions. If h is not too close to 1, namely, $\epsilon \gg \gamma N^{-1}$, they read

$$A_j(t) \simeq \left(\frac{2}{|E'''(\varphi_0)|t}\right)^{\frac{1}{3}}\mathrm{Ai}\left[-N\frac{t-jt_{\rm th}}{t_{\rm th}}\left(\frac{2}{|E'''(\varphi_0)|t}\right)^{\frac{1}{3}}\right]\times\cos(E(\varphi_0)t-jN\varphi_0),$$

$$B_j(t) \simeq \frac{\varepsilon(\varphi_0)}{E(\varphi_0)}\left(\frac{2}{|E'''(\varphi_0)|t}\right)^{\frac{1}{3}}\mathrm{Ai}\left[-N\frac{t-jt_{\rm th}}{t_{\rm th}}\left(\frac{2}{|E'''(\varphi_0)|t}\right)^{\frac{1}{3}}\right]\times\sin(E(\varphi_0)t-jN\varphi_0), \quad (26)$$

where $\mathrm{Ai}(x)$ is the Airy function of the first kind and φ_0 corresponds to the maximal group velocity. Curiously enough, the above approximation works well even far from $jt_{\rm th}$. Note that as long as $E'''(\varphi_0)$ does not depend on time, in contrast to $E''(\varphi_{1,2})$, it is much easier in practice to calculate the r.h.s. of Eqs. (26) than the r.h.s. of Eqs. (24) and (25). The only disadvantage of approximation (26) is that we do not analytically control the errors of this approximation; however, numerical calculations show that they are small.

To summarize, in order to approximate the autocorrelation function up to $(s+1)t_{\rm th}$, one should take A_0, B_0 according to Eq. (D7), A_j, B_j with $j = 1,2,\ldots,s-1$ according to Eqs. (24) and (25), and A_s, B_s according to Eq. (26). The resulting expression approximates the autocorrelation function with excellent precision as shown in Fig. 5.

The case where $h \simeq 1$ is, as usual, more cumbersome. We do not provide a complete analysis, which would be

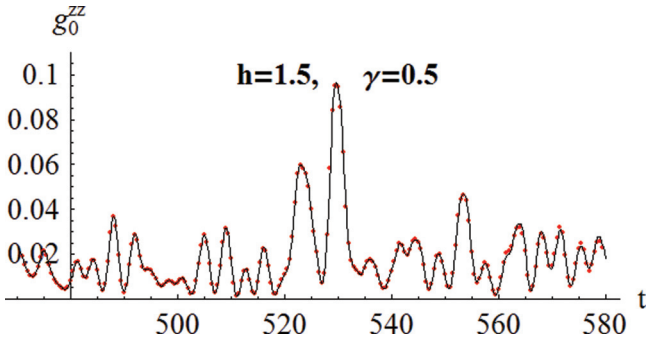

FIG. 5. (Color online) Exact autocorrelation function $g_0^{zz}(t)$ (solid line) and the approximation corresponding to five complete round-trips over a circle [filled (red) circles]. One can see that the approximation excellently describes both the revival and the irregular evolution far from the revival.

rather bulky, however, we derive an approximation for $h = 1$, $\gamma^2 \geqslant 3/4$ [see Appendix D 2c, Eqs. (D32)–(D36)].

Let us discuss the law which governs the decrease in revival amplitudes. In general, the sth partial revival is described by the the mutual interference between all $A_j(t)$ with $j = 0,1,\ldots,s$ and mutual interference between all $B_j(t)$ with $j = 0,1,\ldots,s$. However, as a first approximation one may consider only $A_s(t)$ and $B_s(t)$, which give the leading contribution. Equation (26) tells us that the amplitude of the revivals decreases as $t^{-1/3}$. The average value of g_0^{zz} between revivals decreases more rapidly, namely, as $t^{-1/2}$, according to Eq. (24). This makes the revivals very visible against the background. For $h - 1 > \gamma/N$ one gets the following law from Eq. (26):

$$g_0^{zz}\big|_{s'\text{th revival}} \sim (sN)^{-2/3}. \tag{27}$$

This law works satisfactory for a sufficiently large number of spins and for moderate s. In particular, since the long-time average of g_0^{zz} is of the order of N^{-1}, this law cannot be valid for $s \gtrsim \sqrt{N}$. In fact it breaks down somewhat earlier because, at large s, contributions from A_j, B_j with $j < s$ start to play a role. Our numerical calculations show that for 10 000 spins the above law is reliable for a few dozens of revivals. For a more moderate number of spins, $N \sim 100$, the law is quickly distorted due to the above-mentioned contribution from $A_j(t)$ and $B_j(t)$ with $j < s$. In particular, maxima of revivals do not decrease monotonically in this case (see Fig. 6).

Noteworthily, when $h = 1$ and $\gamma^2 = 3/4$ the amplitudes of the revivals decrease even more slowly than implied by Eq. (27), namely,

$$g_0^{zz}\big|_{s'\text{th revival}} \sim (sN)^{-2/5}, \quad h = 1, \quad \gamma^2 = 3/4; \tag{28}$$

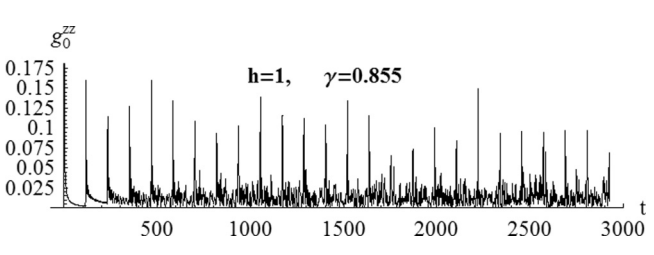

FIG. 6. Extremely pronounced revivals occur in an otherwise erratic regime in a small region of the parameter space in the vicinity of the point $h = 1$, $\gamma^2 = 3/4$. The threshold time here is $t_{\text{th}} \simeq 117$.

see Appendix D 2a and, especially, Eq. (D36) for the details. Again, this law works for a sufficiently large number of spins. However, the fact that the $h = 1$, $\gamma^2 = 3/4$ point of a parameter space is a special one reveals itself already for the modest $N \sim 100$: the revivals appear to be especially pronounced in the vicinity of this point (see Fig. 6), although they do not decrease monotonically due to the above-discussed interference of A_j, B_j with different j. A very similar effect was observed in [19]. Namely, it was numerically discovered that when one initially polarizes a spin at the edge of an open-ended XY chain and allows the excitation to propagate to another edge, the attenuation of the amplitude of a wave packet is minimal for $h = 1$, $\gamma \simeq 0.7$.

V. TRANSITION FROM REGULAR TO ERRATIC EVOLUTION

Plots of $g_0^{zz}(t)$ presented in the present paper clearly demonstrate that the transition from regular to erratic evolution is a general feature of spin dynamics. In the present section we provide a discussion of this fact on the qualitative level. A more thorough study including quantitative considerations will be presented elsewhere.

From Fig. 2 it is evident that the spin evolution is apparently regular at small times but erratic (we are tempted to say "apparently chaotic") at long times, the threshold time t_{th} determining the relevant time scale. However, it is not so easy to define the terms "regular" and "erratic" rigorously in the present context. One should especially be cautious when using the term "chaos" here. A widely used definition of quantum chaos is based on energy level repulsion (see, e.g., [20]). According to this definition the XY model is certainly *not* chaotic because it is integrable and thus its level statistics is Poissonian (i.e., nonrepulsive). In what follows we briefly discuss two distinct approaches which may be used to describe the level of irregularity of $g_0^{zz}(t)$.

The first approach is based on the physical picture of winding of the wave packet over the circle and exploits asymptotic approximations derived above. In this approach we pragmatically consider the evolution to be regular at some interval of time if the correlation function can be well approximated by a linear combination of a *few* ($\ll N$) oscillating functions with different frequencies (probably multiplied by a power-law prefactor) in this interval. Conversely, the evolution is considered to be erratic when the approximation involves many ($\sim N$) harmonics. The first stage of evolution ($t < t_{\text{th}}$) is the most regular one: according to Eqs. (21) and (22) it is described by a single cosine. At times t_{th}, $2t_{\text{th}}$, and $3t_{\text{th}}$ new functions A_j, B_j come into play in Eq. (12) and the number of harmonics increases stepwise. Thus the level of irregularity also increases. This does not last forever: according to Eq. (10), N harmonics is enough to describe $g_0^{zz}(t)$ *exactly*. Evidently the largest possible level of irregularity is achieved no later than at $t = Nt_{\text{th}}$. Note that here we use the term "harmonics" in a slightly nonstandard way: we do not demand that the corresponding frequencies should be multiples of a single, minimal frequency. The described approach resembles the Feigenbaum rout to chaos through period doubling (see, e.g., [21]). However, in the case under consideration there is no *doubling*: the relation between frequencies of new harmonics switching on at certain

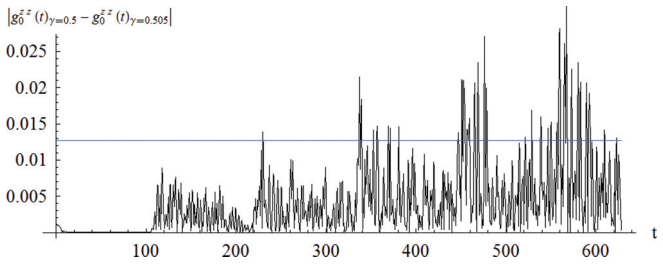

FIG. 7. (Color online) Sensitivity of the correlation function to a small variation of γ. The function plotted is the absolute value of difference of two correlation functions $g_0^{zz}(t)$ corresponding to two slightly different values of the anisotropy parameter: $|g_0^{zz}(t)_{\gamma=0.5} - g_0^{zz}(t)_{\gamma=0.505}|$. The magnetic field in both cases is $h = 1$; the number of spins $N = 100$. The threshold time is approximately 112. The horizontal (blue) line shows the value which the above difference would admit if the two functions were absolutely uncorrelated.

times is not as evident. Moreover, these frequencies may even be slowly varying in time. A Fourier analysis of the correlation function at different time intervals is necessary to obtain a more quantitative picture. This will be done elsewhere.

In the second approach one examines the level of sensitivity of $g_0^{zz}(t)$ to small variations in the Hamiltonian parameters h and γ. This approach, introduced in [22], resembles the definition of classical chaos through the extreme sensitivity to initial conditions. We visualize the sensitivity of $g_0^{zz}(t)$ to small variations of γ in Fig. 7. One can see that during the regular stage of evolution ($t < t_{\rm th}$) such sensitivity is small, while at long times ($t >$ a few $t_{\rm th}$) it is comparable to what one would expect if two correlation functions with slightly different parameters were absolutely mutually uncorrelated. As in the previous approach, the extent of thus defined irregularity increases stepwise at times which are multiples of $t_{\rm th}$, the first step, occurring at $t = t_{\rm th}$, being especially pronounced (see Fig. 7). Curiously, our numerical experiments indicate that the sensitivity of $g_0^{zz}(t)$ to variations of h and γ generically tends to be larger in the vicinity of the QPT line $h = 1$. It would be quite surprising if this relation between the QPT and the sensitivity to small perturbations of the Hamiltonian is confirmed, since the correlation function is calculated at infinite temperature while QPT occurs at zero temperature.

VI. SUMMARY

Numerical studies of the evolution of spin polarization in a finite cyclic XX chain [7] revealed the following physical picture (see also [6,12–14]).

(1) A threshold time exists up to which the polarization of a given spin evolves as if the chain were infinite. This is the time necessary for the fastest spin wave to make a round-trip over the cyclic chain. Up to the threshold time the evolution is regular.

(2) At the threshold time the regular evolution is interrupted by a partial revival. Subsequent partial revivals occur at $2t_{\rm th}, 3t_{\rm th}, \ldots$. Generically the evolution becomes more and more irregular (erratic) after each partial revival.

In the present paper we analytically justify this picture and generalize it to the anisotropic XY chain by developing a method to calculate the infinite-temperature correlation function for long times and beyond the thermodynamic limit. Our core result is as follows.

We express the autocorrelation function $g_0^{zz}(t)$ as a series in winding number j. An appealing feature of this representation is that the jth term does not contribute to the sum until $t = jt_{\rm th}$ and produces a partial revival at $t = jt_{\rm th}$. Each term in the series is defined in integral form. In two special cases ($\gamma = 0$ and $\gamma = 1, h = 1$) it can be expressed through Bessel functions. In a general case we provide very accurate explicit approximations valid at various times and in various regions of parameter space. Thus tractable approximations for $g_0^{zz}(t)$ at long times are obtained.

Other related results are as follows.

(1) The parameter dependence of the threshold time $t_{\rm th}$ is analyzed.

(2) The asymptotic law of the revival amplitude decrease is established. This is a direct application of the above core result. For the bulk of the model parameter space the law has the form $\sim(jN)^{-2/3}$ (with j being the number of the revival), however, for special values of parameters it can be altered. In particular, in the vicinity of the point $h = 1, \gamma^2 = 3/4$ the law has the form $\sim(jN)^{-2/5}$, which leads to extremely pronounced revivals.[3]

(3) We show that a spin distinguished by the initialization retains the memory of this fact forever. In particular, its polarization [proportional to $g_0^{zz}(t)$] never changes sign and its time-averaged polarization differs from the time-averaged polarization of any other spin.[4] Thus we encounter the absence of complete thermalization, which is, however, only a finite-size effect (scaling as $1/N$).[5]

A striking feature of the dynamics in the finite spin chain is the transition from regular to erratic behavior. In the present paper we have restricted ourselves to a brief and qualitative discussion of the nature and origin of this transition. Further work is necessary to give a more exhaustive and quantitative analysis.

ACKNOWLEDGMENTS

The authors acknowledge the enlightening comments by J. H. H. Perk and L. Banchi and the fruitful discussion at the Condensed Matter Theory seminar at ITAE RAS, especially the valuable remarks made by A. L. Rakhmanov concerning signatures of onset of erratic behavior in the XY model. O.L. also thanks E. Bogomolny and O. Giraud for useful discussions. O.L. is grateful to the ERC (Grant No. 279738 NEDFOQ) for financial support. The partial support from Grants No. NSh-4172.2010.2, No. RFBR-11-02-00778, and

[3]Such pronounced revivals were previously observed numerically in an open-ended chain [19].

[4]See [7] for analogous conclusions in the context of the XX model.

[5]In the thermodynamic limit the time-averaged polarization of any spin is 0, in agreement with both the Gibbs distribution and the *generalized* Gibbs distribution (which takes into account the integrals of motion; see, e.g., [23,24]). The reason for this agreement is that our system is effectively at infinite temperature. Thus our work cannot contribute to the ongoing debate about what the correct equilibrium state of an integrable system is.

No. RFBR-10-02-01398 and from the Ministry of Education and Science of the Russian Federation under Contracts No. 02.740.11.5158 and No. 02.740.11.0239 is also acknowledged.

APPENDIX A: DIAGONALIZATION OF A FINITE CYCLIC *XY* SPIN CHAIN

1. Ranges of parameters

Let us rewrite the Hamiltonian we are going to diagonalize:

$$H(h,\gamma,\kappa) = \frac{\kappa}{4}\sum_{n=1}^{N}\left((1+\gamma)\sigma_n^x\sigma_{n+1}^x + (1-\gamma)\sigma_n^y\sigma_{n+1}^y\right) + \frac{h}{2}\sum_{n=1}^{N}\sigma_n^z, \tag{A1}$$

where indices 1 and $N+1$ are identified, and N is even. Here we have introduced coupling constant κ, which is taken to be 1 everywhere in the article except this subsection. Let us show that one may consider $h,\gamma,\kappa \geqslant 0$ without loss of generality. This means that one can change the sign of each constant by means of local unitary transformation U. These transformations correspond merely to rotations of the coordinate systems at each spin site.

To change the sign of h one can transform $\sigma_n^y \to -\sigma_n^y$, $\sigma_n^z \to -\sigma_n^z$ at each spin site n:

$$U = \prod_{n=1}^{N} e^{i\sigma_n^x\pi/2} = \prod_{n=1}^{N} i\sigma_n^x,$$

$$U^\dagger\sigma_n^x U = \sigma_n^x, \quad U^\dagger\sigma_n^y U = -\sigma_n^y, \tag{A2}$$

$$U^\dagger\sigma_n^z U = -\sigma_n^z, \quad U^\dagger H(h,\gamma,\kappa)U = H(-h,\gamma,\kappa).$$

Analogously, to change the sign of γ one transforms $\sigma_n^x \to \sigma_n^y$, $\sigma_n^y \to -\sigma_n^x$ at each site n by means of $U = \prod_{n=1}^{N} e^{i\sigma_n^z\pi/4}$.

To change the sign of κ one transforms $\sigma_{2m}^x \to -\sigma_{2m}^x$, $\sigma_{2m}^y \to -\sigma_{2m}^y$ at each *even* site $2m$ by means of $U = \prod_{m=1}^{N/2} e^{i\sigma_{2m}^z\pi/2}$. As soon as the sign of κ is unimportant, one may put $\kappa = 1$.

2. H in terms of $\sigma_n^\pm$

We define the operators $\sigma_n^\pm$ in the usual way:

$$\sigma_n^+ = \tfrac{1}{2}\left(\sigma_n^x + i\sigma_n^y\right), \quad \sigma_n^- = \tfrac{1}{2}\left(\sigma_n^x - i\sigma_n^y\right). \tag{A3}$$

These operators are neither Bose nor Fermi operators:

$$\sigma_n^+\sigma_n^- + \sigma_n^-\sigma_n^+ = 1, \tag{A4}$$

$$\sigma_m^+\sigma_n^- = \sigma_n^-\sigma_m^+ \quad \text{for} \quad m \neq n. \tag{A5}$$

The following simple equalities prove to be useful:

$$\sigma^z = 2\sigma^+\sigma^- - 1 = -2\sigma^-\sigma^+ + 1, \tag{A6}$$

$$\sigma^z\sigma^+ = -\sigma^+\sigma^z = \sigma^+, \quad \sigma^z\sigma^- = -\sigma^-\sigma^z = -\sigma^-. \tag{A7}$$

The Hamiltonian may be rewritten in terms of $\sigma_n^\pm$ as follows:

$$H = H_0 + H_\gamma + H_h, \tag{A8}$$

with

$$H_0 = \frac{1}{2}\sum_{n=1}^{N}(\sigma_n^+\sigma_{n+1}^- + \sigma_n^-\sigma_{n+1}^+), \tag{A9}$$

$$H_\gamma = \frac{\gamma}{2}\sum_{n=1}^{N}(\sigma_n^+\sigma_{n+1}^+ + \sigma_n^-\sigma_{n+1}^-), \tag{A10}$$

$$H_h = h\sum_{n=1}^{N}\sigma_n^+\sigma_n^- - Nh/2. \tag{A11}$$

3. Jordan-Wigner transformation

Define the operators,

$$\Pi_n \equiv \prod_{n=1}^{n}\sigma_n^z. \tag{A12}$$

Evidently, Π_N coincides with the parity operator Π defined in Sec. II.

Define Fermi operators a_n^- and a_n^+ as follows:

$$a_n^- \equiv \sigma_n^-\Pi_{n-1} = \Pi_{n-1}\sigma_n^-, \quad a_n^+ \equiv \sigma_n^+\Pi_{n-1} = \Pi_{n-1}\sigma_n^+. \tag{A13}$$

This implies

$$\sigma_n^- = a_n^-\Pi_{n-1} = \Pi_{n-1}a_n^-, \quad \sigma_n^+ = a_n^+\Pi_{n-1} = \Pi_{n-1}a_n^+, \tag{A14}$$

$$\{a_m^+,a_n^-\} = \delta_{mn}, \quad \{a_m^+,a_n^+\} = \{a_m^-,a_n^-\} = 0, \tag{A15}$$

$$\sigma_n^z = 2a_n^+a_n^- - 1 = -2a_n^-a_n^+ + 1. \tag{A16}$$

The Hamiltonian takes the form (note that now the ordering of $a_n^\pm$, $a_{n+1}^\pm$ is important; also note the change of the total sign)

$$H_0 = -\frac{1}{2}\left[\sum_{n=1}^{N}(a_n^+a_{n+1}^- + a_{n+1}^+a_n^-) - (1+\Pi)(a_N^+a_1^- + a_1^+a_N^-)\right], \tag{A17}$$

$$H_\gamma = -\frac{\gamma}{2}\left[\sum_{n=1}^{N}(a_n^+a_{n+1}^+ + a_{n+1}^-a_n^-) - (1+\Pi)(a_N^+a_1^+ + a_1^-a_N^-)\right], \tag{A18}$$

$$H_h = h\sum_{n=1}^{N}a_n^+a_n^- - Nh/2. \tag{A19}$$

4. Fourier transformation

Define for arbitrary real q

$$b_q^- \equiv \frac{e^{i\pi/4}}{\sqrt{N}}\sum_{n=1}^{N}e^{-2\pi iq(n-1)/N}a_n^-, \quad b_q^+ \equiv \frac{e^{-i\pi/4}}{\sqrt{N}}\sum_{n=1}^{N}e^{2\pi iq(n-1)/N}a_n^+. \tag{A20}$$

Then

$$\{b_k^+,b_q^+\}=\{b_k^-,b_q^-\}=0,\quad \{b_k^+,b_q^-\}=\frac{1}{N}\frac{1-e^{2\pi i(k-q)}}{1-e^{2\pi i(k-q)/N}}. \tag{A21}$$

In particular, if one takes

$$q=-\frac{N}{2}+1,\quad -\frac{N}{2}+2,\ldots,\frac{N}{2}\quad (X_{\rm odd}) \tag{A22}$$

or

$$q=-\frac{N}{2}+\frac{1}{2},\quad -\frac{N}{2}+\frac{3}{2},\ldots,\frac{N}{2}-\frac{1}{2}\quad (X_{\rm ev}), \tag{A23}$$

then the set of b_q^- is the set of Fermi annihilation operators.

The Hamiltonian may be written in terms of $b_q^\pm$ as follows:

$$H=H^{\rm odd}P^{\rm odd}+H^{\rm ev}P^{\rm ev}, \tag{A24}$$

with

$$P^{\rm odd}\equiv(1-\Pi)/2,\quad P^{\rm ev}\equiv(1+\Pi)/2, \tag{A25}$$

$$H^{\rm ev}=\sum_{q=1/2}^{N/2-1/2}H_q,\quad H^{\rm odd}=\sum_{q=1}^{N/2-1}H_q+H_{0,N/2}, \tag{A26}$$

$$\begin{aligned}H_q&=(h-\cos\varphi(q))(b_q^+b_q^-+b_{-q}^+b_{-q}^-)\\&\quad+\gamma\sin\varphi(q)(b_q^+b_{-q}^++b_{-q}^-b_q^-)-h,\quad \varphi(q)\equiv 2\pi q/N,\end{aligned} \tag{A27}$$

and

$$H_{0,N/2}=(h-1)b_0^+b_0^-+(h+1)b_{N/2}^+b_{N/2}^--h. \tag{A28}$$

5. Bogolyubov transformation

Define the following quantities:

$$\Gamma_q\equiv\gamma\sin\varphi(q),\quad \varepsilon_q\equiv h-\cos\varphi(q),\quad E_q\equiv\sqrt{\varepsilon_q^2+\Gamma_q^2}. \tag{A29}$$

Each H_q may be written as follows:

$$H_q=(\,b_q^+\ \ b_{-q}^-\,)\begin{pmatrix}\varepsilon_q & \Gamma_q\\ \Gamma_q & -\varepsilon_q\end{pmatrix}\begin{pmatrix}b_q^-\\ b_{-q}^+\end{pmatrix}. \tag{A30}$$

It is possible to diagonalize this matrix through Bogolyubov transformation:

$$c_q^-=\cos\frac{\theta_q}{2}b_q^-+\sin\frac{\theta_q}{2}b_{-q}^+. \tag{A31}$$

The diagonalization condition reads $\tan\theta_q=\Gamma_q/\varepsilon_q$, and we choose

$$\theta_q\equiv\arctan\frac{\Gamma_q}{\varepsilon_q}\quad\text{for all}\quad q\neq 0. \tag{A32}$$

This transformation preserves the anticommutation relations. $H_{0,N/2}$ requires special treatment, which leads to $\theta_{N/2}=0$,

$$\theta_0=\begin{cases}0, & h\geqslant 1,\\ \pi, & 0\leqslant h<1.\end{cases} \tag{A33}$$

The inverse transformation reads

$$b_q^-=\cos\frac{\theta_q}{2}c_q^--\sin\frac{\theta_q}{2}c_{-q}^+. \tag{A34}$$

The odd and even parts of the Hamiltonian take the form

$$H^{\rm odd(ev)}=\sum_{q\in X_{\rm odd(ev)}}E_q\left(c_q^+c_q^--\frac{1}{2}\right). \tag{A35}$$

This completes the diagonalization.

6. Eigenstates

Let us first prove the existence of the Fock vacuum states with respect to the annihilation operators c_q^-, i.e., the states $|{\rm vac}\rangle_{\rm odd},|{\rm vac}\rangle_{\rm ev}$ which satisfy

$$c_q^-|{\rm vac}\rangle_{\rm odd(ev)}=0\ \ \forall q\in X_{\rm odd(ev)}. \tag{A36}$$

Evidently it is sufficient to prove that

$$\prod_{q\in X_{\rm odd(ev)}}c_q^-\neq 0. \tag{A37}$$

If this condition is fulfilled, one can always choose some states $|\Psi_{\rm odd(ev)}\rangle$ and normalization constants $\aleph_{\rm ev}$ such that

$$|{\rm vac}\rangle_{\rm odd}=\aleph_{\rm odd}c_{-N/2+1}^-c_{-N/2+2}^-\ldots c_{N/2}^-|\Psi_{\rm odd}\rangle, \tag{A38}$$

$$|{\rm vac}\rangle_{\rm ev}=\aleph_{\rm ev}c_{-N/2+1/2}^-c_{-N/2+3/2}^-\ldots c_{N/2-1/2}^-|\Psi_{\rm ev}\rangle. \tag{A39}$$

The equality

$$\left\{c_{-N/2+1}^+,\left[c_{-N/2+2}^+,\left\{\ldots,\left\{c_{N/2-1}^+,\left[c_{N/2}^+\prod_{q\in X_{\rm odd}}c_q^-\right]\right\}\ldots\right\}\right]\right\}=1 \tag{A40}$$

and the analogous equality for $q\in X_{\rm odd(ev)}$ prove Eq. (A37). Note that $|{\rm vac}\rangle_{\rm ev}$ is indeed an eigenstate of the Hamiltonian, while $|{\rm vac}\rangle_{\rm odd}$ is not.

All the eigenstates of the Hamiltonian are obtained from the vacuum states by applying the creation operators c_q^+. To create an odd number of fermions one should use $q\in X_{\rm odd}$ and $|{\rm vac}\rangle_{\rm odd}$, while to create an even number of fermions one should use $q\in X_{\rm ev}$ and $|{\rm vac}\rangle_{\rm ev}$.

Evidently one can enumerate all the eigenstates of the Hamiltonian by the multiindexes

$$Q_M\equiv\{q_1,q_2,\ldots,q_M\},\quad 0\leqslant M\leqslant N, \tag{A41}$$

with the ordering $q_1<q_2<\cdots<q_M$. Then an eigenstate with M fermions reads

$$|Q_M\rangle\equiv c_{q_M}^+\ldots c_{q_2}^+c_{q_1}^+|{\rm vac}\rangle_{\rm odd(ev)}, \tag{A42}$$

with $q_1,q_2,\ldots,q_M\in X_{\rm odd(ev)}$ when M is odd (even). The corresponding eigenenergy reads

$$E_{Q_M}\equiv\sum_{q\in Q_M}E_q-\frac{1}{2}\sum_{q\in X_{\rm odd(ev)}}E_q. \tag{A43}$$

For our purposes we need only the matrix elements between states with the same parity, therefore we use the notation $|{\rm vac}\rangle$ without subscripts in what follows.

APPENDIX B: CALCULATION OF $g_n^{zz}(t)$

To calculate the correlation function at infinite temperature,

$$g_n^{zz}(t) = 2^{-N} \sum_{Q,\tilde{Q}} \langle Q|\sigma_1^z|\tilde{Q}\rangle\langle\tilde{Q}|\sigma_{n+1}^z|Q\rangle e^{-i(E_Q - E_{\tilde{Q}})t}, \quad \text{(B1)}$$

one needs to calculate the corresponding matrix elements. To do this one uses

$$\begin{aligned} a_{n+1}^+ a_{n+1}^- = \frac{1}{N}\sum_{p,\tilde{p}} &\cos\frac{\theta_{\tilde{p}}}{2}\sin\frac{\theta_p}{2} c_{\tilde{p}}^+ c_p^+ e^{-2\pi i(p+\tilde{p})n/N} \\ &+ \sin\frac{\theta_{\tilde{p}}}{2}\cos\frac{\theta_p}{2} c_{\tilde{p}}^- c_p^- e^{2\pi i(p+\tilde{p})n/N} \\ &+ \cos\frac{\theta_{\tilde{p}}}{2}\cos\frac{\theta_p}{2} c_{\tilde{p}}^+ c_p^- e^{2\pi i(p-\tilde{p})n/N} \\ &+ \sin\frac{\theta_{\tilde{p}}}{2}\sin\frac{\theta_p}{2} c_{\tilde{p}}^- c_p^+ e^{-2\pi i(p-\tilde{p})n/N}. \end{aligned} \quad \text{(B2)}$$

Here $p, \tilde{p}$ can run either through X_{odd} or through X_{ev}; the expression is valid in both cases. Now it can easily be seen that only three types of matrix elements do not vanish.

(1) Diagonal matrix elements:

$$\langle Q|\sigma_{n+1}^z|Q\rangle = \frac{1}{N}\sum_{p\in X_M} \eta(Q_M, p)\cos\theta_p. \quad \text{(B3)}$$

Here $\eta(Q_M, p) = 1$ if $p \in Q_M$ and -1 otherwise; $X_M = X_{\text{odd(even)}}$ if M is odd(even).

(2) Matrix elements between two states with an equal number of fermions, differing by one fermion momentum:

$$\begin{aligned} &Q_M = K_{M-1}\cup\{p\}, \quad \tilde{Q}_M = K_{M-1}\cup\{\tilde{p}\}, \\ &p, \tilde{p} \notin K_{M-1}, \quad p \neq \tilde{p}: \\ &\langle\tilde{Q}|\sigma_{n+1}^z|Q\rangle = e^{2\pi i(p-\tilde{p})n/N}\frac{2}{N}\cos\frac{\theta_p + \theta_{\tilde{p}}}{2}\langle\tilde{Q}|c_{\tilde{p}}^+ c_p^-|Q\rangle, \end{aligned} \quad \text{(B4)}$$

where $\langle\tilde{Q}|c_{\tilde{p}}^+ c_p^-|Q\rangle = \pm 1$, depending on the signature of the corresponding permutation. Note that this sign is not important for calculation of $g_n^{zz}(t)$.

(3) Matrix elements between two states one of which can be obtained from another by the addition of two fermions:

$$\begin{aligned} &Q_M = \tilde{Q}_{M-2}\cup\{p\}\cup\{\tilde{p}\}, \quad p, \tilde{p} \notin \tilde{Q}_{M-2}, \quad p \neq \tilde{p}: \\ &\langle\tilde{Q}|\sigma_{n+1}^z|Q\rangle = \langle Q|\sigma_{n+1}^z|\tilde{Q}\rangle^* \\ &\qquad = -\frac{2}{N}e^{2\pi i(p+\tilde{p})n/N}\sin\frac{\theta_p - \theta_{\tilde{p}}}{2}\langle\tilde{Q}|c_{\tilde{p}}^- c_p^-|Q\rangle. \end{aligned} \quad \text{(B5)}$$

Now let us sum in Eq. (B1) separately over each type of matrix element.

(1) Summation over $Q = \tilde{Q}$ gives

$$\begin{aligned} 2^{-N}\left(\frac{1}{N^2}\sum_{p,\tilde{p}\in X_{\text{odd}}}\cos\theta_p\cos\theta_{\tilde{p}}\sum_{\text{odd}M}\sum_{Q_M}\eta(Q,p)\eta(Q,\tilde{p})\right. \\ \left. + \{\text{odd}\to\text{even}\}\right) = \frac{1}{2N^2}\left(\sum_{p\in X_{\text{odd}}} + \sum_{p\in X_{\text{ev}}}\right)\cos^2\theta_p. \end{aligned} \quad \text{(B6)}$$

(2) Summation over pairs $(Q, \tilde{Q})$ of the form $Q = K\cup\{p\}, \tilde{Q} = K\cup\{\tilde{p}\}$ gives

$$\begin{aligned} &\frac{1}{2N^2}\left(\sum_{\substack{p,q\in X_{\text{odd}}\\ p\neq\tilde{p}}} + \sum_{\substack{p,q\in X_{\text{ev}}\\ p\neq\tilde{p}}}\right)e^{2\pi i(p-\tilde{p})n/N - i(E_p - E_{\tilde{p}})t} \\ &\quad\times\cos^2\frac{\theta_p + \theta_{\tilde{p}}}{2}. \end{aligned} \quad \text{(B7)}$$

(3) Summation over pairs $(Q, \tilde{Q})$ of the form $Q = K\cup\{p\}\cup\{\tilde{p}\}, \tilde{Q} = K$ gives

$$\begin{aligned} &\frac{1}{4N^2}\left(\sum_{p,q\in X_{\text{odd}}} + \sum_{p,q\in X_{\text{ev}}}\right)e^{2\pi i(p+\tilde{p})n/N - i(E_p + E_{\tilde{p}})t} \\ &\quad\times\sin^2\frac{\theta_p - \theta_{\tilde{p}}}{2}, \end{aligned} \quad \text{(B8)}$$

while summation over $Q = K, \tilde{Q} = K\cup\{p\}\cup\{\tilde{p}\}$ gives a complex conjugated contribution.

If one takes $p = q$ in expression (B7), it becomes equal to the (B6) contribution. Exploiting this, one readily obtains

$$\begin{aligned} g_n^{zz}(t) = \frac{1}{2N^2}&\left(\sum_{p,q\in X_{\text{odd}}} + \sum_{p,q\in X_{\text{ev}}}\right) \\ &\times\left(\cos\left(\frac{2\pi(p-\tilde{p})n}{N} - (E_p - E_{\tilde{p}})t\right)\cos^2\frac{\theta_p + \theta_{\tilde{p}}}{2}\right. \\ &\left. + \cos\left(\frac{2\pi(p+\tilde{p})n}{N} - (E_p + E_{\tilde{p}})t\right)\sin^2\frac{\theta_p - \theta_{\tilde{p}}}{2}\right). \end{aligned} \quad \text{(B9)}$$

It can be straightforwardly verified that this expression leads to Eqs. (10) and (11).

Equation (B9) can be used to find a long-time average of the autocorrelation function $\overline{g_0^{zz}} \equiv \lim_{T\to\infty} T^{-1}\int_0^T g_0^{zz}(t)dt$. Let us assume that there are no degeneracies in E_q other than the mirror degeneracy $E_q = E_{-q}$ (in other words, that $E_q = E_p$ implies $|q| = |p|$). This is a generic case. Then

$$\overline{g_0^{zz}} = \frac{1}{N}\left(1 - \frac{1}{N} + \frac{1}{2N}\left(\sum_{p\in X_{\text{odd}}} + \sum_{p\in X_{\text{ev}}}\right)\cos^2\theta_p\right). \quad \text{(B10)}$$

The term $-1/N$, in parentheses, emerges due to $q = 0, N/2$. The long-time average of the correlation function for $n \neq 0$ can be calculated analogously. In the specific case $\gamma = 0$ the result, (B10), coincides with the expression obtained in [7].

APPENDIX C: GROUP VELOCITY OF SPIN WAVES

In the present section we consider $h \geqslant 0$, $\gamma \in [0,1]$. The group velocity of spin waves reads

$$v(\varphi; h, \gamma) = (h - (1-\gamma^2)\cos\varphi)\sin\varphi / E(\varphi; h, \gamma). \quad \text{(C1)}$$

We are interested mainly in the *maximal* velocity for given values of the parameters h and γ:

$$V(h,\gamma) \equiv \sup_{\varphi} v(\varphi; h, \gamma) = v(\varphi_0; h, \gamma), \quad \text{(C2)}$$

where φ_0 is the supremum point. Due to the symmetry of $E(\varphi)$ we can consider $\varphi \geqslant 0$ without loss of generality. The extremum condition $\partial_\varphi v|_{\varphi_0} = 0$ leads to the fourth-degree polynomial equation

$$P(z) \equiv (1-b)^2 z^4 - 3h(1-b)z^3 + (2b(1-b) + h^2(3-2b))z^2 - h(h^2+b)z - b(1-b) + h^2 b = 0, \tag{C3}$$

with $z = \cos\varphi_0$ and $b \equiv \gamma^2$. We are interested in the real roots of this equation, which lie in the interval $[-1,1]$. Let us show that there is only one such root whenever $h \geqslant 1$ (this fact is important for the application of the method of the steepest descent; see Appendix D). In this case the above equation implies that $z \geqslant 0$, therefore in fact we have to consider the interval $[0,1]$. Since $P(0) > 0$, $P(1) < 0$, and $P(+\infty) = +\infty$, we could have one, two, or three roots in $[0,1]$. If there were two or three roots of $P = 0$ in the considered interval, then the equation $P' = 0$ would have two roots in $[0,1]$. However, the latter equation has no more than one root in the considered interval ($z = \frac{h}{4(1-b)}$). Thus Eq. (C3) has exactly one root in the interval $[0; 1]$ for $h \geqslant 1$.

Let us now consider several important special cases.

Case I. $\gamma = 0$. In this case $\varphi_0 = \pi/2$, $V = 1$.

Case II. $\gamma = 1$. In this case

$$\cos\varphi_0 = \begin{cases} h, & h \leqslant 1, \\ h^{-1}, & h > 1 \end{cases} \tag{C4}$$

and

$$V = \begin{cases} h, & h \leqslant 1, \\ 1, & h > 1, \end{cases} \tag{C5}$$

Case III. $h = 0$ In this case $\cos\varphi_0 = -\sqrt{\frac{\gamma}{1+\gamma}}$, $V = 1-\gamma$.

Case IV. $h = 1$. This is an especially interesting case, as it corresponds to the QPT. Velocity $v(\varphi)$ has a step at $\varphi = 0$, the step height being equal to 2γ. Equation (C3) is simplified to

$$(z-1)^2((b-1)^2 z^2 + (2b^2 - b - 1)z + b^2) = 0. \tag{C6}$$

One should distinguish two cases within this category.

Case IV a: $b \in [3/4, 1]$. In this case the only root that satisfies $|z| \leqslant 1$ is $z = 1$. Thus $\varphi_0 = 0$, $V = \gamma$.

Case IV b: $b \in [0, 3/4)$. In this case $\cos\varphi_0 = \frac{2b+1-\sqrt{4b+1}}{2(1-b)}$. One can substitute this value in Eq. (C1) to obtain an explicit, although bulky, expression for V. One can also find a *minimal* value of V with respect to γ:

$$\inf_{\gamma\in[0,1]} V(1,\gamma) = V(1,\sqrt{2-\sqrt{2}}) = 2(\sqrt{2}-1) = 0.828427\ldots. \tag{C7}$$

In what follows we show that this is the minimal value of V in the whole region $h \geqslant 1$, $\gamma \in [0,1]$.

Case V. $h \to \infty$. In this case $\varphi_0 \to 0$, $V \to 1$.

Let us investigate how $V(h,\gamma)$ varies with h. The derivative over h has a rather simple form:

$$\partial_h V(h,\gamma) = b(1 - h\cos\varphi_0)\sin\varphi_0 / E^3(\varphi_0; h, \gamma). \tag{C8}$$

To calculate it we used that $\partial_h V(h,\gamma) = \partial_h v(\varphi_0; h, \gamma)$ due to the equation $\partial_\varphi v(\varphi_0; h, \gamma) = 0$. The stationary points of $V(h,\gamma)$ with respect to h are given by $\partial_h V = 0$, which leads to $\cos\varphi_0 = 1/h$. We plug the latter equality into Eq. (C3) and obtain

$$(1-\gamma^2)(1-z^2)^2(1-(1-\gamma^2)z^2) = 0. \tag{C9}$$

The only roots that satisfy $|z| \leqslant 1$ are $z = \pm 1$, which correspond to $h = 1$. This point is not extremal because $V(0,\gamma) \leqslant V(1,\gamma) \leqslant V(+\infty,\gamma)$. Thus for any fixed γ maximal group velocity $V(h,\gamma)$ grows monotonically with h, from $1-\gamma$ at $h = 0$ to 1 as $h \to \infty$. As a consequence, if one considers only $h \geqslant 1$, then the minimal value of V is given by Eq. (C7).

APPENDIX D: ASYMPTOTIC EXPRESSIONS

Here we consider in detail asymptotic expressions for spectral functions $A_j(t)$ and $B_j(t)$. Let us explore domains in which $E(\varphi)$ is a univalent analytical function. The branch points of this function are found from the equation $(h - \cos\varphi)^2 + (\gamma\sin\varphi)^2 = 0$. For $h^2 > 1-\gamma^2$ its solutions are $\varphi_{\mathrm{br}\pm}$ and $\varphi^*_{\mathrm{br}\pm}$, where

$$\varphi_{\mathrm{br}\pm} = 2\pi k + i\,\mathrm{arccosh}\left(\frac{h \pm \gamma\sqrt{h^2-(1-\gamma^2)}}{1-\gamma^2}\right), \quad k \in Z. \tag{D1}$$

The domain where $E(\varphi)$ remains a univalent analytical function is the hole complex plane without a row of branch cuts from $\varphi_{\mathrm{br}-}$ to $\varphi_{\mathrm{br}+}$ in the $\mathrm{Im}(\varphi) > 0$ half-plane and a row of branch cuts from $\varphi^*_{\mathrm{br}-}$ to $\varphi^*_{\mathrm{br}+}$ in the $\mathrm{Im}(\varphi) < 0$ half-plane. It is important that $\mathrm{Im}(E(\varphi))$ is positive in quadrants I and III and negative in quadrants II and IV. Functions $E(\varphi)$, $\varepsilon(\varphi)$, and $\exp[-ijN\varphi]$, as well as the integrands in Eq. (13), are 2π periodic functions of $\mathrm{Re}(\varphi)$. Thus we consider the strip $\mathrm{Re}(\varphi) \in (-\pi;\pi]$.

In order to use the method of the steepest descent for the integrals in Eq. (13) we have to find saddle points for the functions

$$\begin{aligned} f_{Aj}(\varphi) &\equiv iE(\varphi)t - ijN\varphi, \\ f_{Bj}(\varphi) &\equiv iE(\varphi)t - ijN\varphi + \ln\frac{\varepsilon(\varphi)}{E(\varphi)}. \end{aligned} \tag{D2}$$

The saddle points are defined by the equations

$$E't - jN = 0 \quad \text{and} \quad iE't - ijN + \left(\ln\frac{\varepsilon}{E}\right)' = 0, \tag{D3}$$

respectively.

1. Asymptotics for spectral functions of zero order

Let us first consider spectral functions of zero order, $A_0(t)$ and $B_0(t)$. There are four saddle points in the strip $\mathrm{Re}(\varphi) \in (-\pi;\pi]$, which, for A_0, read

$$\begin{aligned} &\varphi_1 = 0, \quad \varphi_2 = \pi, \quad \varphi_3 = -i\,\mathrm{arccosh}\frac{h}{1-\gamma^2}, \\ &\varphi_4 = +i\,\mathrm{arccosh}\frac{h}{1-\gamma^2}. \end{aligned} \tag{D4}$$

For B_0 we have exactly the same points $\varphi^B_1 = \varphi_1$ and $\varphi^B_2 = \varphi_2$ and slightly (for $t \gg 1$) shifted points φ^B_3 and φ^B_4:

$$\varphi^B_{3,4} = \mp i\,\mathrm{arccosh}\left(\frac{h}{1-\gamma^2} + c_{3,4}\frac{1}{t} + O\left(\frac{1}{t^2}\right)\right). \tag{D5}$$

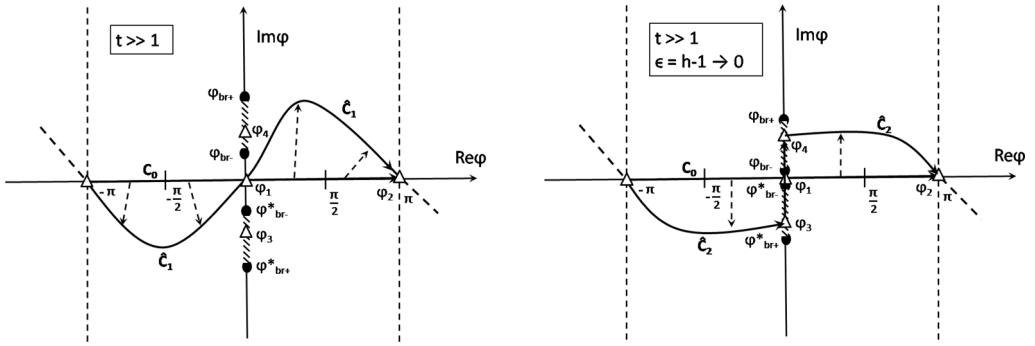

FIG. 8. Integration paths for A_0, B_0 in the case $t \gg 1$, $t \gg \epsilon^{-1}$ (left) and in the case $\epsilon^{-1} \gg t \gg 1$, $\gamma \gg \epsilon$ (right). Open triangles correspond to saddle points; filled circles, to branch points of $E(\varphi)$.

One can find $c_{3,4}$ by substituting $\varphi^B_{3,4} = \varphi_{3,4} + \Delta\varphi$ in the second Eq. (D3). Note that if, in the $(c_{3,4}t^{-1})$ vicinity of $\varphi_{3,4}$, the series for $E(\varphi)$ is convergent, then the difference between φ_3 and $\varphi^B_{3,4}$ is of the order t^{-1}.

Let us define the following parameter:

$$\epsilon \equiv h - 1. \tag{D6}$$

For large enough ϵ we can find asymptotics in the case $t \gg \max\{\epsilon^{-1},1\}$ in a straightforward way. Indeed, we can transform the integration path from our initial C_0 (integration along $\mathrm{Re}(\varphi) = 0$ from $\varphi = -\pi$ to $\varphi = \pi$) to the path $\widetilde{C}_1$, which goes through quadrants I and III, where $\mathrm{Im}(E) > 0$, and through saddle points $\varphi_1 = 0$ and $\varphi_2 = \pi$ (see Fig. 8, left). Then we immediately have

$$\begin{aligned} A_0(t) &\simeq \sqrt{\frac{1}{2\pi t}}\left(a_{0-}\cos\left((h-1)t + \frac{\pi}{4}\right)\right. \\ &\quad \left. + a_{0+}\cos\left((h+1)t - \frac{\pi}{4}\right) + O\left(\frac{1}{t}\right)\right), \\ B_0(t) &\simeq \sqrt{\frac{1}{2\pi t}}\left(a_{0-}\sin\left((h-1)t + \frac{\pi}{4}\right)\right. \\ &\quad \left. + a_{0+}\sin\left((h+1)t - \frac{\pi}{4}\right) + O\left(\frac{1}{t}\right)\right), \end{aligned} \tag{D7}$$

where

$$a_{0\pm} = \sqrt{\frac{h \pm 1}{h \pm (1-\gamma^2)}}$$

and we take into account that $\varepsilon(0)E^{-1}(0) = \varepsilon(\pi)E^{-1}(\pi) = 1$. The region of applicability for large enough ϵ is given by $t \gg 1$, and for $\epsilon \to 0$ we have $t > 2\epsilon^{-1}\ln\frac{1}{\Delta}$, where Δ stays for the value of an error. Under these conditions we have the following approximation for $t < t_{\mathrm{th}}$:

$$g^{zz}_0(t) \simeq \frac{1}{2\pi t}\left((a_{0+} - a_{0-})^2 + 4a_{0+}a_{0-}\cos^2\left(t - \frac{\pi}{4}\right)\right). \tag{D8}$$

Numerical evolution shows an excellent coincidence with the exact solution in the region $1 \ll t < t_{\mathrm{th}}$. Note that this expression becomes asymptotic for $J_0^2(t)$ in the case $\gamma = 0$ (XX chain), which is in accordance with Eq. (17).

Let us consider the case of such small ϵ that $\epsilon \ll \gamma$ and $\epsilon \ll (t)^{-1}$. Since we are interested in the dynamics on a time scale of the order of t_{th} or larger, the latter condition in fact implies that $\epsilon \ll N^{-1} \ll 1$. Now we cannot integrate over the contour $\widetilde{C}_1$ due to the small convergence radius of the series in the vicinity of $\varphi_1 = 0$ (note, however, that the contribution from the saddle point $\varphi_2 = \pi$ remains intact). Therefore we use another integration path, $\widetilde{C}_2$ (see Fig. 8), which goes through saddle points $-\pi$, φ_3, φ_1, and φ_4 and ends up in $\varphi_2 = \pi$. Consider the integration path from φ_3 to φ_4. Integration over branch cuts does not contribute to A_j, B_j (this statement is true for spectral functions of all orders). This is because $\mathrm{Re}(E(\varphi) = 0$ on the branch cuts, and therefore

$$\mathrm{Re}\int_{\mathrm{cut}} e^{itE(\varphi)-in\varphi}d\varphi = \mathrm{Im}\int_{\mathrm{cut}}\frac{\varepsilon(\varphi)}{E(\varphi)}e^{itE(\varphi)-in\varphi}d\varphi = 0. \tag{D9}$$

For small ϵ, branch points can be expanded as $\varphi_{\mathrm{br}-},\varphi^*_{\mathrm{br}-} = \pm i\cdot\epsilon\gamma^{-1} + O(\epsilon^2\gamma^{-2})$. At the segment $[\varphi^*_{\mathrm{br}-},\varphi_{\mathrm{sbr}-}]$ the functions $E(\varphi)$ and $\varepsilon(\varphi)$ are real valued, and $E(\varphi) < \sqrt{2}\epsilon$, $\varepsilon(\varphi)E^{-1}(\varphi) = 1 + O(\epsilon)$, therefore

$$\begin{aligned} &\mathrm{Re}\int_{\varphi^*_{\mathrm{br}-}}^{\varphi_{\mathrm{br}-}} e^{itE(\varphi)}d\varphi < (\sqrt{2}\gamma^{-1}\epsilon + O(\epsilon^2\gamma^{-2}))\cdot\min\{\epsilon t,1\}, \\ &\mathrm{Im}\int_{\varphi^*_{br-}}^{\varphi_{br-}}\frac{\varepsilon(\varphi)}{E(\varphi)}e^{itE(\varphi)}d\varphi = \gamma^{-1}\epsilon + O(\epsilon^2\gamma^{-2}). \end{aligned} \tag{D10}$$

Combining these results with contributions from saddle points φ_2, φ_3, and φ_4, one obtains

$$\begin{aligned} A_0(t) &\simeq \sqrt{\frac{1}{2\pi(2-\gamma^2)t}}\left(\sqrt{2}\cos\left(2t - \frac{\pi}{4}\right)\right. \\ &\quad + (1-\gamma^2)^{\frac{1}{4}}\exp\left[-\frac{\gamma^2}{\sqrt{1-\gamma^2}}t\right] \\ &\quad \left. + O\left(\frac{1}{t}\right) + O(\epsilon\gamma^{-1})\right). \end{aligned} \tag{D11}$$

For B_0, keeping in mind (D5), one obtains

$$\begin{aligned} B_0(t) &\simeq \sqrt{\frac{1}{2\pi(2-\gamma^2)t}}\left(\sqrt{2}\sin\left(2t - \frac{\pi}{4}\right)\right. \\ &\quad + (1-\gamma^2)^{-\frac{1}{4}}\exp\left[-\frac{\gamma^2}{\sqrt{1-\gamma^2}}t\right] \\ &\quad \left. + O\left(\frac{1}{t}\right) + O(\epsilon\gamma^{-1})\right). \end{aligned} \tag{D12}$$

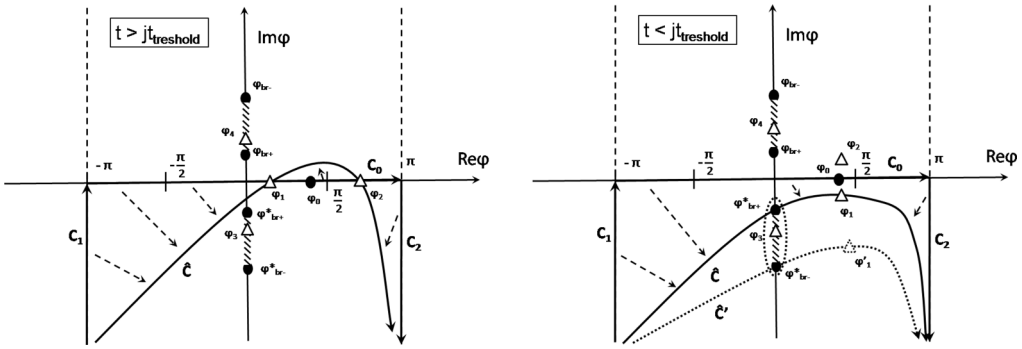

FIG. 9. Integration paths for A_j and B_j in the case $t > jt_{\rm th}$ (left) and in the case $t < jt_{\rm th}$ (right). Open triangles correspond to saddle points; filled circles,s to branch points and to the point φ_0 which satisfies $E(\varphi_0)'' = 0$.

The region of applicability for these asymptotics is limited by the condition that $\exp[-\frac{1}{2}|E''(\varphi_3)|R^2]$ must be small enough [here R is the radius of convergence for $E(\varphi)$ near $\varphi_{3,4}$]. We have $R = |\varphi_3 - \varphi_{\rm br+}| \simeq (2-\sqrt{2})\gamma$ for small γ. Thus we get the following condition of applicability for the above asymptotic:

$$t > (2-\sqrt{2})^{-2}\gamma^{-2}\ln\left(\frac{1}{\Delta}\right), \tag{D13}$$

where Δ is the order of the relative error. Under this condition we can neglect the term $\exp[-\gamma^2(1-\gamma^2)^{-\frac{1}{2}}t]$ in (D11) and (D12). Numerical evaluation shows excellent coincidence of these asymptotics with the exact values of A_0 and B_0 in the case $\gamma \ll 1, t \gg 1$. Moreover, these expressions exactly coincide with asymptotic forms for Bessel functions in (15) in the case $\gamma = 0, h = 1$ which is not obvious from our derivation method. With these remarks, we find

$$\begin{aligned} g_0^{zz}(t) = \frac{1}{\pi(2-\gamma^2)t}\Bigg(1 + \frac{2-\gamma^2}{2\sqrt{1-\gamma^2}}\exp\left[-\frac{2\gamma^2}{\sqrt{1-\gamma^2}}t\right] \\ + 2\sqrt{\frac{2-\gamma^2}{2\sqrt{(1-\gamma^2)}}}\exp\left[-\frac{\gamma^2}{\sqrt{1-\gamma^2}}t\right] \\ \times \cos\left(2t - \frac{\pi}{4} - \arctan\frac{1}{\sqrt{1-\gamma^2}}\right)\Bigg), \end{aligned} \tag{D14}$$

which gives us an excellent approximation for $g_0^{zz}(t)$ in the case $\epsilon \ll \gamma, \epsilon \ll N^{-1}, t < t_{\rm th}$. For not very small γ^2 we can neglect the exponential suppressed terms and obtain

$$g_0^{zz}(t) = \frac{1}{\pi(2-\gamma^2)t}. \tag{D15}$$

2. Asymptotics for spectral functions of nonzero order

For spectral functions of nonzero orders the situation is slightly more complicated. Again, there are four saddle points in the strip $\mathrm{Re}(\varphi) \in (-\pi,\pi]$, but now their positions *vary with time* (see Fig. 9). Consider the function A_j, $j \geqslant 1$. The corresponding saddle points satisfy the four-degree polynomial equation on $z = \cos\varphi$:

$$\begin{aligned} &(1-\gamma^2)^2 z^4 - 2h(1-\gamma^2)z^3 + (h^2 - (1-\gamma^2)^2 \\ &+ \zeta(1-\gamma^2))z^2 + 2h(1-\gamma^2-\zeta)z - h^2 \\ &+ \zeta(h^2+\gamma^2) = 0, \end{aligned} \tag{D16}$$

where $\zeta \equiv (Nj)^2(t)^{-2}$. This equation viewed as the equation for φ gives eight solutions in the strip $\mathrm{Re}(\varphi) \in (-\pi,\pi]$. Four of them are relevant [i.e., are solutions of Eq. (D3)] and thes other four are irrelevant (are solutions of the equation $-E't - jN = 0$). Since $E'(\varphi)$ takes all possible real values on each branch cut, one pair of saddle points, φ_3 and φ_4, lies on two branch cuts symmetrically with respect to the real axis, analogous to the $j = 0$ case.

Let us consider the positions of two other saddle points, φ_1 and φ_2, especially their evolution with time. The definition of the threshold time implies that, for $t < jt_{\rm th}$, Eq. (D3) has no real roots. Thus φ_1 and φ_2 are complex. In fact they are complex conjugate to each other. When time goes on they both approach φ_0, which lies on the real axis, and eventually merge at $t = jt_{\rm th} : \varphi_1(jt_{\rm th}) = \varphi_2(jt_{\rm th}) = \varphi_0$. For $t > jt_{\rm th}$, φ_1 and φ_2 lie on the real axis and move apart from φ_0 and from each other, approaching 0 and π, respectively,as $t \to \infty$.

a. Asymptotics for $t > jt_{\rm th}$

To start with, we warn the reader that we do not provide a strict mathematical proof that a suitable integration path exists which goes through the chosen saddle points in all the presented cases. However, the existence of these paths looks quite natural in all cases, and moreover, the corresponding asymptotic expressions show excellent coincidence with numerical evolutions. Strict mathematical proof is postponed for further work.

With this warning made, let us turn to the case $t > jt_{\rm th}$. We start from the case of nonsmall ϵ and we assume that φ_1 and φ_2 are situated far enough from each other so that we can neglect their mutual influence in the asymptotics. The conditions under which this assumption is fulfilled are considered in what follows.

Note that we can integrate along the path $C_1 \cup C_0 \cup C_2$, where C_0 is the original path, C_1 starts from $\varphi = -\pi - i\infty$ and goes to $\varphi = -\pi$ along $\mathrm{Re}\,\varphi = \mathrm{const} = -\pi$, and C_2 starts from $\varphi = \pi$ and goes to $\varphi = \pi - i\infty$ along $\mathrm{Re}\,\varphi = \mathrm{const} = \pi$ (see Fig. 9). Since $f_{A,Bj}(x+iy)$ are 2π periodic functions of x, the value of the integral along the new path is exactly the same as along C_0. Now we transform the path $C_1 \cup C_0 \cup C_2$ to the path $\widehat{C}$, which starts from $\varphi = -\pi - i\infty$, goes through saddle points φ_1 and φ_2, and ends at $\varphi = \pi - i\infty$ (see Fig. 9, left). There are two topologically different possible integration paths $\widehat{C}$: the first one goes above the branch cut; the second

one, under the cut. In the latter case according to the Cauchy theorem we have to subtract the integral over the branch cut. However, as discussed above this integral does not contribute to A_j and B_j [see Eq. (D9)].

Now we can proceed to find asymptotic expressions as contributions from points φ_1 and φ_2. Under all specified conditions, we immediately obtain Eq. (24) for A_j. For B_j, using reasoning similar to those following Eq. (D5), we get Eq. (25).

Let us now investigate the range of applicability of Eqs. (24) and (25). First, we consider in what cases we can use the standard approximation for the contribution of the saddle points under the assumption that the radius of convergence for corresponding series is large enough. In this case the derived approximation may deviate from the exact expression for two reasons: a small value of $|E(\varphi_{1,2})''|$ and interception of contributions for φ_1 and φ_2 due to their close relative positions. These two features can appear only for small times after jt_{th}. Let us give a more precise estimation without detailed explanations. If $\delta t \equiv t - jt_{\text{th}} > 0$, then it has to be $\frac{\delta t}{t_{\text{th}}} > \sqrt[3]{\frac{j}{2\cdot r\cdot N^2}}$, where $r \equiv \frac{E(\varphi_0)}{|E'''(\varphi_0)|}$ is a quantity of the order of 1 for the vast majority of the Hamiltonian parameter space. One can see that these asymptotic approximations for spectral functions of order j become accurate starting at times close to jt_{th}.

Now let us investigate in what cases series does not converge in a large enough circle for some saddle points. We have to explore small enough ϵ, at least $\epsilon^{-1} \gg t$. Since for a spectral function of order j we are interested in $t > jt_{\text{th}}$, it is useful to consider $\epsilon^{-1} \gg jN$. First, we define the position of φ_0:

$$\varphi_0 = \arccos\left(\frac{2\gamma^2+1-\sqrt{4\gamma^2+1}}{2(1-\gamma^2)}\right) + O(\epsilon), \quad \gamma^2 \leqslant \frac{3}{4},$$
$$\varphi_0 = \frac{2^{\frac{1}{2}}\epsilon^{\frac{1}{2}}}{(4\gamma^2-3)^{\frac{1}{4}}} + O(\epsilon), \quad \gamma^2 > \frac{3}{4}. \tag{D17}$$

Let us consider the case $\gamma^2 < \frac{3}{4}$. For times which satisfy $jt_{\text{th}} < t < j\widetilde{t}_{\text{th}} = jN\gamma^{-1} + O(\epsilon)$ there is no point φ_1 near $\varphi = 0$, and the derived asymptotic expressions, (24) and (25), are valid. If $t > \widetilde{t}_{\text{th}}$ one obtains

$$\varphi_1 = \frac{\epsilon}{\gamma\sqrt{\frac{\gamma^2 t^2}{j^2N^2}-1}} + O(\epsilon^2), \quad t > j\widetilde{t}_{\text{th}} = j\frac{N}{\gamma} + O(\epsilon). \tag{D18}$$

Thus for $t \ll \epsilon^{-1}$ we cannot use the above-derived approximations because φ_1 is situated close to $\varphi_{\text{br}-}$ and the radius of convergence $R = \sqrt{\epsilon^2\gamma^2+\varphi_1^2}$ is very small, $|E''(\varphi_1)|tR^2 < 1$, thus we cannot use the method of the steepest descent for φ_1 (we assume here that $\gamma \gg \epsilon$). Instead we can proceed analogously to the case of spectral functions of zero order. Namely, we move the integration path in order to go through saddle points φ_3 and φ_4 and neglect the value of the integral between $\varphi^*_{\text{br}-}$ and $\varphi_{\text{br}-}$ as we have done in (D7). The difference from the case of A_0 and B_0 is that now we can neglect the exponentially suppressed contribution from φ_3, but the contribution from φ_4 may be not small for some portion of time. Numerical evaluation shows that for $N \gg 1$ the contribution from φ_4 is exponentially suppressed at a time scale $\sim\widetilde{t}_{\text{th}}$. Summarizing, for time $t > \widetilde{t}_{\text{th}}$ we obtain

$$A_j(t) \simeq \frac{1}{\sqrt{2\pi t}}\left(\frac{1}{2}\sqrt{\frac{1}{|E''(\varphi_4)|}}\exp[-t(-iE(\varphi_4+0)) + jN(-i\varphi_4)] + \sqrt{\frac{1}{|E''(\varphi_2)|}} \times \cos\left(tE(\varphi_2) - jN\varphi_2 - \frac{\pi}{4}\right) + O\left(\frac{1}{t}\right)\right), \tag{D19}$$

where one should remember that $-iE(\varphi_4+0) > 0$, $(-i\varphi_4) > 0$. The factor $\frac{1}{2}$ is due to the fact that we have to take only one-half of the contribution from φ_4. Analogously, one obtains

$$B_j(t) \simeq \frac{1}{\sqrt{2\pi t}}\left(\frac{1}{2}\frac{\varepsilon(\varphi_4)}{(-iE(\varphi_4+0))}\sqrt{\frac{1}{|E''(\varphi_4)|}} \times \exp[-t(-iE(\varphi_4+0)) + jN(-i\varphi_4)] + \frac{\varepsilon(\varphi_2)}{E(\varphi_2)} \times \sqrt{\frac{1}{|E''(\varphi_2)|}}\sin\left(tE(\varphi_2) - jN\varphi_2 - \frac{\pi}{4}\right) + O\left(\frac{1}{t}\right)\right). \tag{D20}$$

The only case we do not investigate here is $\gamma \leqslant \epsilon \ll 1$. We leave it for future work.

If $\gamma^2 \geqslant \frac{3}{4}$, then φ_0 is situated in the vicinity of $\varphi = 0$, which leads to $t_{\text{th}} = \widetilde{t}_{\text{th}} = N\gamma^{-1} + O(\epsilon)$. Therefore the asymptotic expressions (D19) and (D20) are valid starting from time t, for which φ_2 is situated far enough from $\varphi = 0$ [the corresponding condition reads $\frac{1}{2}|E''(\varphi_2)|t\varphi_2^2 \gg 1$]. For times in the vicinity of jt_{th} another approximation should be used (see Appendix D2c).

b. Asymptotics for $t < jt_{\text{th}}$

When $t < jt_{\text{th}}$ the path of integration should not go through quadrant I, since for all values of $x \in (-\pi;\pi)$ $\partial_y \text{Re}(iEt - in\varphi) > 0$ (remember that $\varphi = x + iy$). We shift our integration path to $\widetilde{C}$ or $\widetilde{C}'$ (see Fig. 9) and obtain asymptotics from the contribution from only one saddle point, φ_1. For large enough $|\delta t|$, where $\delta t \equiv t - jt_{\text{th}} < 0$, we have

$$A_j(t) \simeq \sqrt{\frac{1}{2\pi|E''(\varphi_1)|t}}\cos\left(E(\varphi_1)t - jN\varphi_1 + \sigma(\varphi_1)\right), \tag{D21}$$

where $\sigma(\varphi_1)$ is the angle between the path and the line $\text{Im}\, f_{A_j} = \text{const}$. Let us evaluate φ_1 approximately for $t \lesssim jt_{\text{th}}$ such that $t^{-1}\delta t \ll 1$. If $E_0''' \equiv E'''(\varphi_0) \neq 0$, then

$$\varphi_1 = \varphi_0 - i\eta + \frac{1}{6}\frac{E_0^{(IV)}}{E_0'''}\eta^2 + i\left(\frac{5}{72}\left(\frac{E_0^{(IV)}}{E_0'''}\right)^2 - \frac{1}{24}E_0^{(V)}\right)\eta^3 + O(\eta^4) + iO(\eta^5), \tag{D22}$$

where

$$\eta \equiv \sqrt{-\frac{2N\delta t}{|E_0'''|t t_{\text{th}}}} = \sqrt{-2r\frac{\delta t}{t}}, \quad r \equiv \frac{E_0'}{|E_0'''|}.M$$

Up to the first order in $\delta t \cdot t^{-1} \simeq \delta t \cdot j^{-1} t_{\rm th}^{-1}$, one obtains

$$A_j(t) \simeq \frac{r^{\frac{1}{4}}(jN)^{\frac{1}{2}}}{2^{\frac{3}{4}}\pi^{\frac{1}{2}}}\left(\frac{-\delta t}{jt_{\rm th}}\right)^{-\frac{1}{4}} \exp\left[\frac{-2\sqrt{2r}}{3} jN\left(\frac{-\delta t}{jt_{\rm th}}\right)^{\frac{3}{2}} + O\left(\left(\frac{-\delta t}{jt_{\rm th}}\right)^{\frac{5}{2}}\right)\right] \cos\left(E(\varphi_0)t - jN\varphi_0\right) + O\left(\left(\frac{-\delta t}{jt_{\rm th}}\right)^{\frac{3}{4}}\right). \tag{D23}$$

This expression gives only the order of suppression; if one is interested in a more precise expression, he has to directly solve Eq. (D3) to find the exact value of φ_1 and substitute it in the general formula, (D21). This formula [and approximation (D23)] is valid until we can neglect the term $\frac{1}{6}E'''(\varphi_1)(\Delta\varphi)^3$ in comparison with $\frac{1}{2}E''(\varphi_1)(\Delta\varphi)^2$ in the series expansion near φ_1. This leads to the condition $jN(\frac{\delta t}{jt_{\rm th}})^{\frac{3}{2}} \gg 1$. In the opposite case, $jN(\frac{\delta t}{jt_{\rm th}})^{\frac{3}{2}} \ll 1$, Eqs. (D3) and (D23) are not valid and the leading order contribution is given by the term $\frac{1}{6}E'''(\varphi_1)(\varphi)^3$, which leads to

$$A_j(t) \simeq \frac{\Gamma\left(\frac{1}{3}\right) r^{\frac{1}{3}}}{2^{\frac{2}{3}} 3^{\frac{1}{6}} \pi j^{\frac{1}{3}} N^{\frac{1}{3}}} \cdot \left(\frac{|E(\varphi_0)'''|t_{\rm th}}{|E(\varphi_1''')|t}\right)^{\frac{1}{3}} \cdot \cos(E(\varphi_1)t - jN\varphi_1), \tag{D24}$$

where the values of $E(\varphi_1)$ and $E(\varphi_1''')$ can be found according to Eq. (D22). Equations (D24) and (D23) become asymptotics for $J_j(t)$ in the case of the XX chain. If one wants to derive asymptotics valid in the region $jN(\frac{\delta t}{jt_{\rm th}})^{\frac{3}{2}} \sim 1$, one has to calculate the integral through the saddle point with the proper path direction [here we use approximation (D22) for saddle points],

$$I_{\rm saddle}(t) \simeq \int \exp\left[-\frac{1}{2}\eta|E_0'''|tz^2 - \frac{i}{6}|E_0'''|tz^3\right]dz, \tag{D25}$$

and use the formula

$$A_j(t) \simeq \frac{1}{2\pi} I_{\rm saddle}(t) \exp\left[\frac{-2\sqrt{2r}}{3} jN\left(\frac{-\delta t}{jt_{\rm th}}\right)^{\frac{3}{2}}\right] \times \cos(E(\varphi_0)t - jN\varphi_0). \tag{D26}$$

Equations (D23) and (D24) can be obtained from the above formula by neglecting the second summand in the exponent in (D25) and by expanding the integrand in Eq. (D25) in powers of η.

Let us turn to B_j. In order to describe its behavior in an analogous way, one should start from

$$B_j(t) \simeq \mathrm{Im}\left(\sqrt{\frac{1}{2\pi|E''(\varphi_1)|t}}\frac{\varepsilon(\varphi_1)}{E(\varphi_1)} \exp[iE(\varphi_1)t - ijN\varphi_1 + i\sigma(\varphi_1)]\right) \tag{D27}$$

instead of (D21). We do not describe $B_j(t)$ in detail because there is no simple approximation formula for (D27) for all possible values of $\cos(\varphi_0)$. However, the exponential suppression for $B_j(t)$ has the same form as that for $A_j(t)$; only the pre-exponential factor differs. This is because the suppression is determined by the exponent of the quantity $-\mathrm{Re}(-iE(\varphi_1)t + ijN\varphi_1)$, which is the same for B_j and A_j up to t^{-1}.

To conclude this subsection, the suppression of spectral functions $A_j(t)$ and $B_j(t)$ with $\delta t = t - jt_{\rm th} < 0$, with exponential precision, reads

$$A_j(t) \sim B_j(t) \sim \exp\left[-\frac{2}{3}\sqrt{\frac{2E'(\varphi_0)}{|E'''(\varphi_0)|}} jN\left(\frac{-\delta t}{jt_{\rm th}}\right)^{\frac{3}{2}} + O\left(\left(\frac{\delta t}{jt_{\rm th}}\right)^{\frac{5}{2}}\right)\right]. \tag{D28}$$

This is in accordance with a general result [17]. Here we assume that $E'''(\varphi_0) \neq 0$; for very small $E'''(\varphi_0)$ one has to take into account $E^{(IV)}(\varphi_0)$, which leads to a slightly different law.

c. *Asymptotics for $t \simeq jt_{\rm th}$*

The considerations in the present subsection are less rigorous than in the previous ones. The only consequence, however, is that we do not completely control errors for derived approximations. Numerical calculations demonstrate that the latter are, nevertheless, rather accurate over a wide range of model parameters. For certain regions of the parameter space in which the derived approximations fail we are able to identify the reason and point out the way to overcome the difficulties.

Let us describe the method. When $t \simeq t_{\rm th}$ the saddle points are situated near φ_0. The integrand is a very rapidly oscillating function for all φ except $\varphi \simeq \varphi_0$. Thus the value of the integral is picked up on a small segment $[\varphi_0 - \Delta\varphi; \varphi_0 + \Delta\varphi]$, $\Delta\varphi > \frac{1}{2}(\varphi_2 - \varphi_1)$. In order to estimate errors for this approximation, one has to make bulky calculations in the spirit of the above subsections. We avoid this in the present work.

In order to calculate the integral along the small segment, we expand $E(\varphi)$ in the vicinity of φ_0. And the last approximation is to replace the interval of integration from $[-\Delta\varphi, \Delta\varphi]$ to $[-\infty; \infty]$, where the integration variable is $\mu \equiv \varphi - \varphi_0$. The latter trick is justified because our new integrand oscillates as $\sim\exp(i \cdot \mathrm{const} \cdot \mu^3)$ when $\mu \to \pm\infty$. All these approximations are legitimate when the model parameters are such that φ_0 is far enough from points of branching. Thus the approximation is valid for large enough ϵ and all values of γ and for $\epsilon \ll 1$ it is valid for $\gamma^2 < \frac{3}{4}$. Let us assume that $E_0''' \equiv E'''(\varphi_0)$ is not very small. In this case one can consider the power expansion of $E(\varphi)$ up to $(\varphi - \varphi_0)^3$ and neglect terms $\sim O((\varphi - \varphi_0)^4)$. Thus for $t \simeq jt_{\rm th}$ one gets

$$\begin{aligned} A_j(t) &= \frac{1}{2\pi}\int_{-\pi}^{\pi} \cos(Et - jN\varphi)d\varphi \\ &\simeq \frac{1}{2\pi}\int_{-\Delta\varphi}^{\Delta\varphi} \cos\left(E_0 t - jN\varphi_0 + (E_0' t - jN)\mu - \frac{1}{6}|E_0'''|t\mu^3\right)d\mu \\ &\simeq \left(\frac{2}{|E_0'''|t}\right)^{\frac{1}{3}} \frac{1}{2\pi}\int_{-\infty}^{\infty} \cos\left[(E_0 t - jN\varphi_0) - \frac{t - jt_{\rm th}}{t_{\rm th}}N \times \left(\frac{2}{|E_0'''|t}\right)^{\frac{1}{3}}\xi + \frac{1}{3}\xi^3\right]d\xi. \end{aligned} \tag{D29}$$

Here all functions f with subindex 0 should be understood as $f_0 \equiv f(\varphi_0)$. The above integral is a well-known Airy function of the first kind:

$$\mathrm{Ai}(x) \equiv \frac{1}{\pi}\int_0^\infty \cos\left(\frac{\xi^3}{3}+x\xi\right)d\xi. \tag{D30}$$

Thus we get Eq. (26) (with analogous reasoning for B_j).

Let us investigate now the case $h=1$, $\gamma^2 > \frac{3}{4}$ (we do not investigate here the case of small, but nonzero $\epsilon = h-1 \ll 1$). For $h=1$, $\gamma^2 > \frac{3}{4}$ we cannot use formula (D29), since $\varphi_0 = \varphi_{\mathrm{br}-} = \varphi^*_{\mathrm{br}-} = 0$. But we can argue that the main contribution for A_j is picked up on the segment $[0,\varphi]$, since only on this segment the oscillation frequency is not very high (note that for $[-\Delta\varphi,0]$ the frequency is high; this is due to the discontinuity of the group velocity at $\varphi = 0$). If we somehow expand $E(\varphi)$ on $[0,\varphi]$, we can obtain a good approximation. Consider $-E(\varphi)$ on a complex plain. If we have values for $E(\varphi)$ on the segment $\varphi \in [0,\pi]$ fixed, we can make analytical continuation to $\mathrm{Re}(\varphi) \in [-\pi,0]$ in two ways: with the branch cut $\mathrm{Re}(\varphi_{\text{branch cut}}) = 0$, $\mathrm{Im}(\varphi_{\text{branch cut}}) \in [-\varphi^*_{\mathrm{br}+},\varphi_{\mathrm{br}+}]$ and with the branch cut $\mathrm{Re}(\varphi_{\text{branch cut}}) = 0$, $\mathrm{Im}(\varphi_{\text{branch cut}}) \in [-\infty, -\varphi^*_{\mathrm{br}+}] \cup [\varphi_{\mathrm{br}+},\infty]$. In the first case we have our original function $E(\varphi)$ in the segment $\varphi \in [-\pi,0]$. In the second case we have some new function $\widetilde{E}(\varphi)$ which does not coincide with $E(\varphi)$ in this segment. But in the latter case we can use power expansion for $\widetilde{E}(\varphi)$ in the circle with radius $R = |\varphi_{\mathrm{br}+}|$:

$$\widetilde{E}(\varphi) = \gamma\varphi + \frac{3-4\gamma^2}{24\gamma}\varphi^3 + \frac{16\gamma^4-15}{1920\gamma^3}\varphi^5 + O(\varphi^7). \tag{D31}$$

Analogously to (D29), one obtains

$$A_j(t) \simeq \frac{1}{2\pi}\int_0^\infty \cos\left[(\gamma t - jN)\varphi + \frac{3-4\gamma^2}{24\gamma}t\varphi^3 + \frac{16\gamma^4-15}{1920\gamma^3}t\varphi^5\right]d\varphi. \tag{D32}$$

If one can neglect the term $\sim\varphi^5$ (i.e., if $\gamma^2 - \frac{3}{4}$ is large enough), one gets

$$A_j(t) \simeq \frac{1}{2}\left(\frac{2\gamma}{(\gamma^2-\frac{3}{4})t}\right)^{\frac{1}{3}} \cdot \mathrm{Ai}\left[-(\gamma t - jN)\left(\frac{2\gamma}{(\gamma^2-\frac{3}{4})t}\right)^{\frac{1}{3}}\right], \quad h=1, \quad \gamma^2 > \frac{3}{4}. \tag{D33}$$

For B_j one uses power expansion $\varepsilon(\varphi)E^{-1}(\varphi)$ in the vicinity of $\varphi = 0$ to obtain

$$B_j(t) \simeq \frac{1}{4\gamma}\left(\frac{2\gamma}{(\gamma^2-\frac{3}{4})t}\right)^{\frac{2}{3}} \cdot \mathrm{Ai}'\left[-(\gamma t - jN)\left(\frac{2\gamma}{(\gamma^2-\frac{3}{4})t}\right)^{\frac{1}{3}}\right], \quad h=1, \quad \gamma^2 > \frac{3}{4}, \tag{D34}$$

where the prime indicates the derivative.

Let us consider the special case $h=1$, $\gamma^2 = \frac{3}{4}$. We have $t_{\mathrm{th}} = \frac{2}{\sqrt{3}}N$. The term $\sim\varphi^3$ in power expansion $\widetilde{E}(\varphi)$ is 0: $\widetilde{E}(\varphi) = \frac{\sqrt{3}}{2}\varphi - \frac{1}{120\sqrt{3}}\varphi^5$. Let us introduce the function

$$\mathrm{gAi}_n(x) \equiv \frac{1}{\pi}\int_0^\infty \cos\left(\frac{\xi^n}{n}+x\xi\right)d\xi. \tag{D35}$$

The Airy function of the first kind is a particular case of this function: $\mathrm{Ai}(x) = \mathrm{gAi}_3(x)$. $\mathrm{gAi}_n(x)$ for $n > 3$ exhibits the same behavior as $\mathrm{Ai}(x)$: for positive x it is exponentially decreasing, and for negative x it oscillates and goes to 0 when $x \to -\infty$. A_j and B_j are expressed through this function and its derivative:

$$A_j(t) \simeq \frac{1}{2}\left(\frac{24\sqrt{3}}{t}\right)^{\frac{1}{5}} \cdot \mathrm{gAi}_5\left[-\left(\frac{\sqrt{3}t}{2} - jN\right)\left(\frac{24\sqrt{3}}{t}\right)^{\frac{1}{5}}\right], \quad h=1, \quad \gamma^2 = \frac{3}{4};$$

$$B_j(t) \simeq \frac{1}{4\gamma}\left(\frac{24\sqrt{3}}{t}\right)^{\frac{2}{5}} \cdot \mathrm{gAi}'_5\left[-\left(\frac{\sqrt{3}t}{2} - jN\right)\left(\frac{24\sqrt{3}}{t}\right)^{\frac{1}{5}}\right], \quad h=1, \quad \gamma^2 = \frac{3}{4}. \tag{D36}$$

Note that the rather small value of the coefficient of term φ^5 in the power expansion of $\widetilde{E}(\varphi)$ implies that these approximations work well for sufficiently long times ($t \gg 24\sqrt{3}$). Analogously, we require $t \gg 2\gamma(\gamma^2 - \frac{3}{4})^{-1}$ in Eqs. (D33) and (D34). Note that if one wishes to investigate approximations which successfully describe A_j, B_j near the threshold time in the region of parameter space $h=1$, $\gamma^2 \simeq \frac{3}{4}$, then one has to calculate integral (D32) saving both terms, $\sim\varphi^3$ and $\sim\varphi^5$. Therefore, in this case there is no such clear power law for the time dependence of the maximum value of the spectral function as in (D37).

Now let us discuss possible values of maxima for A_j and B_j. If jN is sufficiently large the positions of global maxima of A_j and B_j coincide with those for $\mathrm{Ai}(x)$ and $\mathrm{gAi}_5(x)$:

$$\sup_t A_j(t) \simeq \left(\frac{2}{|E'''_0|t}\right)^{\frac{1}{3}} \cdot a_3, \quad \text{for } h>1, \text{ or } h=1, \gamma^2 < \frac{3}{4};$$

$$\sup_t A_j(t) \simeq \frac{1}{2}\left(\frac{2\gamma}{(\gamma^2-\frac{3}{4})t}\right)^{\frac{1}{3}} \cdot a_3, \quad \text{for} \quad h=1, \quad \gamma^2 > \frac{3}{4};$$

$$\sup_t A_j(t) \simeq \frac{1}{2}\left(\frac{24\sqrt{3}}{t}\right)^{\frac{1}{5}} \cdot a_5, \quad \text{for} \quad h=1, \quad \gamma^2 = \frac{3}{4}. \tag{D37}$$

Here a_3 and a_5 are global maxima of $\mathrm{Ai}(x)$ and $\mathrm{gAi}_5(x)$ ($a_3 = 0{,}54,\ldots, a_5 = 0.44,\ldots$), respectively. Without loss of precision one can replace t with jt_{th} in the above expressions. We do not present the analogous expressions for $B_j(t)$ because the positions of the maxima of these functions obviously do not coincide with those for A_j [when $A_j(t)$ achieves the global maximum $B_j(t)$ becomes 0]. In the last two cases in Eq. (D37) it is A_j^2 which gives the main contribution to $g_0^{zz}(t)$ near $t = jt_{\mathrm{th}}$. When $h>1$ or $h=1$, $\gamma^2 < \frac{3}{4}$ one has to investigate the maximum of $A_j(t)^2 + B_j(t)^2$ in order to find the leading contribution to $g_0^{zz}(t)$. This leads to

$$\mathrm{Max}_{(\mathrm{revival}j)}\left[g_0^{zz}(t)\right] \simeq 4\left(\frac{2}{|E'''_0|jt_{\mathrm{th}}}\right)^{\frac{2}{3}} \cdot \left(1 + \left|\frac{\varepsilon_0}{E_0} - 1\right|\right)a_3^2, \quad \text{for} \quad h>1, \quad \text{or} \quad h=1, \quad \gamma^2 < \frac{3}{4};$$

$$\mathrm{Max}_{(\mathrm{revival}j)}\left[g_0^{zz}(t)\right] \simeq \left(\frac{2\gamma^2}{\left(\gamma^2-\frac{3}{4}\right)jN}\right)^{\frac{2}{3}}\cdot a_3^2, \quad \text{for } h=1,\ \gamma^2>\frac{3}{4};$$
$$\mathrm{Max}_{(\mathrm{revival}j)}\left[g_0^{zz}(t)\right] \simeq \left(\frac{36}{jN}\right)^{\frac{2}{5}}\cdot a_5^2, \quad \text{for } h=1,\ s\gamma^2=\frac{3}{4}. \tag{D38}$$

Note that this is a rather rude approximation, since interference terms may be large. Therefore these expressions work well only for a large number of spins. Numerical evolution shows that the revivals are maximally pronounced for $h=1$ and γ^2 slightly less than $\frac{3}{4}$. This may be expected on the basis of Eq. (D32).

Let us emphasize once more that all the derived expressions can be derived with more rigor using integrals in the complex plain, analogous to what was done in the previous subsections.

We have not explored the whole parameter space. In particular, we have not considered the cases $h=1$, $\gamma^2\simeq\frac{3}{4}$, $\epsilon=h-1\ll 1$, $\epsilon\neq 0$, or $h>1$, $E_0'''=0$. Some of the derived approximations work well only for long times and, correspondingly, large numbers of spins [for example, $t\gg 24\sqrt{3}$ or $t\gg 2\gamma(\gamma^2-\frac{3}{4})^{-1}$]. However, for a large region of parameter space these approximations work fairly well, and they provide an opportunity to investigate amplitudes of maxima in partial revivals or, at least, the law of their decrease. For these reasons we decided to include in the paper these not completely rigorous calculations. The validity of formulas derived in the present subsection is justified by the fact that approximations (26) give the same result as the more rigorously derived Eqs. (D23) and (D24) when the ranges of applicability overlap.

[1] D. Porras and J. I. Cirac, Phys. Rev. Lett. **92**, 207901 (2004).
[2] S. Bose, Phys. Rev. Lett. **91**, 207901 (2003).
[3] E. Lieb, T. Schultz, and D. Mattis, Ann. Phys. **16**, 407 (1961).
[4] P. Mazur and T. J. Siskens, Physica **69**, 259 (1973).
[5] T. J. Siskens and P. Mazur, Physica **71**, 560 (1974).
[6] E. B. Fel'dman, R. Bruschweiler, and R. R. Ernst, Chem. Phys. Lett. **294**, 297 (1998).
[7] E. B. Fel'dman and M. G. Rudavets, Chem. Phys. Lett. **311**, 453 (1999).
[8] R. Bruschweiler and R. R. Ernst, Chem. Phys. Lett. **264**, 393 (1997).
[9] J. Mossel and J.-S. Caux, New J. Phys. **12**, 055028 (2010).
[10] O. Lychkovskiy, J. Phys.: Conf. Ser. **306**, 012028 (2011).
[11] J. Häppölä, G. B. Halász, and A. Hamma, Phys. Rev. A **85**, 032114 (2012).
[12] Z. Zhu, A. Aharony, O. Entin-Wohlman, and P. C. E. Stamp, Phys. Rev. A **81**, 062127 (2010).
[13] V. A. Benderskii and E. I. Kats, JETP Lett. **94**, 459 (2011).
[14] V. A. Benderskii and E. I. Kats, J. Exp. Theor. Phys. **116**, 1 (2013).
[15] V. A. Benderskii, A. S. Kotkin, and E. I. Kats, Phys. Lett. A **377**, 737 (2013).
[16] T. Niemeijer, Physica **36**, 377 (1967).
[17] E. H. Lieb and D. W. Robinson, Commun. Math. Phys. **28**, 251 (1972).
[18] L. Banchi, T. J. G. Apollaro, A. Cuccoli, R. Vaia, and P. Verrucchi, Phys. Rev. A **82**, 052321 (2010).
[19] A. Bayat, L. Banchi, S. Bose, and P. Verrucchi, Phys. Rev. A **83**, 062328 (2011).
[20] F. Haake, *Quantum Signatures of Chaos*, Vol. 54 (Springer-Verlag, Berlin, 2010).
[21] M. Feigenbaum, Los Alamos Sci. **1**, 4 (1980).
[22] A. Peres, *Quantum Theory: Concepts and Methods*, Vol. 57 (Kluwer Academic, Dordrecht, 1993).
[23] L. D. Landau and E. M. Lifshits, *Statistical Physics*, Part 1, Vol. 5 (Pergamon Press, London, 1980).
[24] M. Rigol, V. Dunjko, V. Yurovsky, and M. Olshanii, Phys. Rev. Lett. **98**, 050405 (2007).